Available online at www.sciencedirect.com
ScienceDirect
ELSEVIER
Mathematical and Computer Modelling xx (xxxx) xxx–xxx
MATHEMATICAL AND COMPUTER MODELLING
www.elsevier.com/locate/mcm

A two-scale model for an array of AFM's cantilever in the static case

M. Lenczner*, R.C. Smith

Center for Research in Scientific Computation, North Carolina State University, Raleigh, NC 27695, United States

Received 13 July 2006; accepted 3 December 2006

Abstract

The primary objective of this paper is to present a simplified model for an array of Atomic Force Microscopes (AFMs) operating in static mode. Its derivation is based on the asymptotic theory of thin plates initiated by P. Ciarlet and P. Destuynder and on the two-scale convergence introduced by M. Lenczner which generalizes the theory of G. Nguetseng and G. Allaire. As an example, we investigate in full detail a particular configuration, which leads to a very simple model for the array. Aspects of the theory for this configuration are illustrated through simulation results. Finally the formulation of our theory of two-scale convergence is fully revisited. All the proofs are reformulated in a significantly simpler manner.

Keywords: Atomic force microscopy; Microsystems arrays; Multiscale modeling; Homogenization

1. Introduction

In recent years, a number of new Microsystem or Nanosystem Array architectures have been developed. These architectures include microcantilevers, micromirrors, droplet ejectors, micromembranes, microresistors, biochips, nanodots, nanowires to cite only a few, and applications are continually emerging in numerous areas of science and technology. In some of these systems, units have a collective behavior whereas in others they are working individually. However, in all cases their coupling is an important design parameter of the array that is promoted or avoided. The coupling can be of various natures, including mechanical, thermal and electromagnetic. The numerical simulation of such whole arrays based on classical methods like the Finite Element Method (FEM) is prohibitive for today's computers at least in a time compatible with the time scale of a designer. Indeed, the calculation of a reasonably complex cell of a three-dimensional microsystem requires about 10^3 degrees of freedoms which leads to about 10^7 degrees of freedoms for a 100×100 array. Moreover usual microsystems involve strong nonlinearities that cannot be ignored.

This work is focused on a relatively simple example of a Microsystem Array, namely an Atomic Force Microscope Array (AFMA). A number of developments of AFMAs or of more simple Cantilever Arrays have already been achieved, as noted in the abbreviated set of citations [29–62].

The modeling of a single AFM has been extensively studied in the literature in many different configurations, as noted in the review papers [14,21,13]. Most of the models are based on a spring–damper–mass model where the

* Corresponding address: UTBM-M3M, Center for Research in Scientific Computation, 90010, Belfort, Cedex, France.
E-mail addresses: michel.lenczner@utbm.fr (M. Lenczner), rsmith@eos.ncsu.edu (R.C. Smith).

0895-7177/$ - see front matter © 2007 Elsevier Ltd. All rights reserved.
doi:10.1016/j.mcm.2006.12.028

precise features of the mechanical systems are ignored. More careful modeling has been derived in various situations including tapping mode, interaction with a surrounding fluid; see [16–23]. They are based on the Euler–Bernoulli beam model with an applied force at the extremity of the beam, except in [12], where the tip is modeled as a rigid part and the force is applied to it. Until now, to the best of our knowledge, only the group of B. Bamieh (see [24] and the reference therein) has published a model of a coupled cantilever array. These authors take into account the electrostatic coupling with a rudimentary derivation.

To simplify the discussion we focus on the simplest case of an AFMA in static operation. We establish a two-dimensional thin plate model for an elastic component including a rigid part corresponding to the tip that is assumed to be much stiffer than the supple part of the cantilever. Then a simplified model of an array of AFMs coupled through their base is derived from the thin plate model. Each of these models is illustrated by an example. Analytic calculations are conducted to yield very simple formulations. Finally a numerical simulation of the array is presented and discussed. The derivations of the two models are rigorously justified through asymptotic methods. The thin plate model is based on the asymptotic methods of Ciarlet [2] and Destuynder [1] as well as on our previous work [6]. The derivation of the AFMA two-scale model uses the two-scale transform and convergence introduced by one of the authors; see [15,11] and [10]. However, it is completely reformulated in a simpler and more intuitive manner.

We note that, for the geometry considered in this paper, our two-scale convergence is equivalent to the two-scale convergence of Nguetseng [7] and Allaire [5]. However, it is worthwhile remarking that it has the of working also for electrical circuit homogenization (as a particular case of $d - n$ dimensional periodic manifolds immersed in a d-dimensional space) when the other does not apply as it has also been recognized in [9]. This remark constitutes an encouragement to develop this method in the framework of Mechatronical Systems. We point out that these methods are in the vein of the homogenization methods by Sanchez-Palencia [3], L. Tartar and Bensoussan, Lions, Papanicolaou [4]. Finally, we cite the work of Griso and his coworkers initiated in [8], who have rediscovered the same method and named it the Unfolding Method.

We review the main features of the simplified models presented in this paper. Simply stated, an AFM evaluates the interaction force between the tip and the sample through the deformation measurement of the supple part of the cantilever. To do so, the tip is designed so that its deformation is very weak so that it efficiently transmits the energy of deformation. This is why we assume that the tip is perfectly rigid. This assumption simplifies the model significantly by reducing the number of degrees of freedom. Then, the thin plate model is derived under the assumption that on the one side the supple part of the cantilever is very thin and at the same time that the tip is also thin, both with the same order of magnitude. The AFMA is constituted of cantilevers clamped in a common base. For the model derivation, we assume that the base is much stiffer than the cantilever. This is expressed by saying that their stiffnesses have different asymptotic behavior. Doing this, the effective stiffness of the base in the homogenized model is not affected by the presence of the cantilever and so is independent of the tip–sample forces (that produce nonlinearities). This is an appreciable simplification. In the example that we detail, the base and the cantilevers are rectangular. The tip–sample forces are the van der Waals forces and the chemical interaction forces. In this case the model is on the one side a fourth-order one-dimensional boundary value problem related to the deflection in the base coupled with the model of the cantilever at the microscale which reduces to a single nonlinear algebraic equation related to the tip–sample distance. The numerical simulations are conducted for simple sample profiles: flat, slope and a quadratic shape. The tip–sample distance is a distributed variable along the array that we discretize with Chebychev polynomials. The numerical experiments show that, even for simple sample shapes, a relatively large number of polynomials are required for an accurate approximation. It is also observed that even for a moderate number of cantilevers the deflection of the base is far from being negligible in comparison with the tip displacement. This is due to the fact that the deflection increases when the length of the base increase as its fourth power.

We note that the derivation of a two-scale model for the evolution problem can be directly deduced from the static model. However, the dynamic problem requires much dedicated analysis, simulations and discussions so that we have chosen to postpone its presentation until a further publication.

The paper is organized as follows. We establish aspects of the geometry and the nature of tip forces in the remainder of this section. The three-dimensional elastic model coupled with a rigid part is stated and derived in Section 2. The thin plate model is stated and derived in Section 3. The two-scale model is stated and derived in Section 4. It is based on the two-scale theory presented in the Appendix A. The examples and the numerical simulations are reported in Section 6.

Please cite this article in press as: M. Lenczner, R.C. Smith, A two-scale model for an array of AFM's cantilever in the static case, Mathematical and Computer Modelling (2007), doi:10.1016/j.mcm.2006.12.028

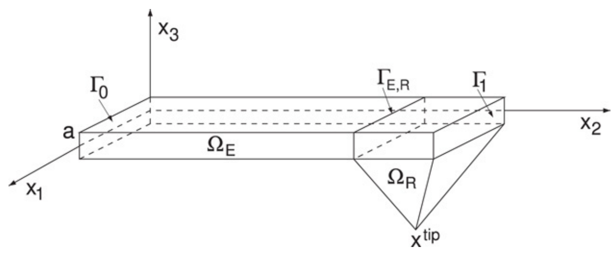

Fig. 1. Three-dimensional plate with the rigid part.

2. Three-dimensional model

We start by considering a mechanical structure located in $\Omega \subset \mathbb{R}^3$ made up of an elastic part and a rigid part located respectively in Ω_E and in Ω_R as depicted in Fig. 1. The model is stated in the next section and subsequently justified in Section 2.2.

2.1. Statement of the model

The elastic component is clamped along part of its boundary Γ_0, is linked to the rigid part through the interface $\Gamma_{E,R}$ and is free of applied forces in the remaining part Γ_1. When the system is totally elastic (no rigid part), then Ω_R and $\Gamma_{E,R}$ are void and the related equation must be ignored. The mechanical displacements are denoted by the vector $u = (u_1, u_2, u_3)^T$ defined over the entire structure.

The fourth-order elasticity tensor is denoted by R and may vary in space if the material is not homogeneous. The symmetric matrix of linear strains is $s(u) = \frac{1}{2}(\nabla u + \nabla^T u)$, where ∇ is the gradient operator. The equilibrium equations, the linear stress–strain relation and the rigidity constraint are stated as

$$-\mathrm{div}(\sigma) = f, \quad \sigma = Rs(u) \text{ in } \Omega_E \text{ and } s(u) = 0 \text{ in } \Omega_R \tag{1}$$

where the product between the fourth-order tensor R and the matrix $s(u)$ gives the 3×3 matrix with entries

$$\sigma_{ij} = \sum_{k,l=1}^{3} R_{ijkl} s_{kl}(u).$$

In the case of isotropic elasticity, the elasticity tensor has the form

$$R_{ijkl} = \lambda \delta_{ij} \delta_{kl} + 2\mu \delta_{ik} \delta_{jl}$$

where δ is the Kronecker delta.

The boundary conditions are $u = 0$ on Γ_0, $\sigma n = 0$ on Γ_1 (n being the outward normal vector to the boundary). Moreover, u will be continuous at the interface $\Gamma_{E,R}$. Finally, the force and force momentum transmissions satisfy

$$\int_{\Gamma_{E,R}} \sigma n \mathrm{d}s = \xi, \quad \int_{\Gamma_{E,R}} (\sigma n).(x \times e_k) \mathrm{d}s = \Xi_k \quad \text{for } k \in \{1, 2, 3\} \tag{2}$$

where

$$\xi = \int_{\Omega_R} f(x) \mathrm{d}x, \quad \Xi_k = \int_{\Omega_R} f(x).(x \times e_k) \mathrm{d}x.$$

We note that the condition $s(u) = 0$ can be formulated through imposing a rigid displacement $u = b + x \times B$ whose b and B are some three-dimensional vectors. The variational formulation, which is necessary for the formulation of Galerkin-like numerical methods, can be formulated as follows: find $u \in V$ such that

$$\int_{\Omega_E} \sigma :: s(v) \mathrm{d}x = \int_{\Omega} f.v \mathrm{d}x \tag{3}$$

for all $v \in V$ for the previous stress–strain relationship where the admissible space of test functions is

$$V = \{v \in H^1(\Omega)^3 / s(v) = 0 \text{ in } \Omega_R \text{ and } v = 0 \text{ on } \Gamma_0\}.$$

The Sobolev space $H^1(\Omega)$ is the set of square integrable functions in Ω, $\int_\Omega v^2(x)\mathrm{d}x < \infty$, such that each component of their gradient is also square integrable.

2.2. Justification of the three-dimensional model

Consider a sequence of elastic structures filling up Ω so that its rigidity in Ω_R tends to infinity. Namely, the sequence of elasticity tensors has the form $R^n = R$ in Ω_E and $R^n = nR$ in Ω_R, where n varies in $\mathbb{N}^*$ from one to infinity. The variational formulation of such a sequence of elastic problem is as follows: find $u^n \in V_E$

$$\int_\Omega [R^n s(u^n)] :: s(v)\mathrm{d}x = \int_\Omega f.v\mathrm{d}x$$

for all $v \in V_E$ where

$$V_E = \{v \in H^1(\Omega)^3 / v = 0 \text{ on } \Gamma_0\}.$$

Using classical estimates, one may prove that $\|\nabla u^n\|^2_\Omega$ and $n\|s(u^n)\|^2_{\Omega_R}$ are bounded uniformly with respect to n where $\|v\|^2_\Omega = \int_\Omega v^2(x)\mathrm{d}x$.

The use of these estimates justifies the expansion $u^n = u + O(1/n)$ with u independent of n and satisfying $s(u) = 0$ in Ω_R. Taking n to infinity in the variational formulation and posing $v = 0$ in Ω_R, it follows that u solves the variational formulation (3). The derivation of the local form of the variational formulation (3) is routine and is not detailed here.

3. A thin plate model

The cantilever of an AFM is comprised of a thin plate equipped with a tip as depicted in Fig. 1. The thin plate is assumed to be elastic and the tip is modeled by a rigid body. A simplified model, based on the classical Love–Kirchhoff elastic thin plate theory, is stated in the forthcoming section and its justification is made in Section 3.2.

3.1. Statement of the model

Because the elastic component is a thin elastic plate with thickness $2a$ and mean section ω_E, we consider the domain

$$\Omega_E = \{x \in \mathbb{R}^3 / (x_1, x_2) \in \omega_E, -a < x_3 < a\}. \tag{4}$$

The three parts Γ_0, Γ_1 and $\Gamma_{E,R}$ of its boundary are parameterized in a similar manner by referring to the corresponding boundaries γ_0^P, γ_1^P and $\gamma_{E,R}^P$ of ω_E. The rigid part is parameterized as

$$\Omega_R = \{x \in \mathbb{R}^3 / (x_1, x_2) \in \omega_R \text{ with } -h(x_1, x_2) < x_3 < a\}. \tag{5}$$

When a is small enough the three-dimensional model can be simplified to a thin plate model. To justify it, we make some assumptions on the order of magnitude of the applied forces with respect to the thickness a:

$$f_{\alpha=1,2} = O(1), \qquad a^{-1} f_3 = O(1) \quad \text{in } \Omega \quad \text{and} \quad a^{-1} h = O(1) \quad \text{in } \Omega_R. \tag{6}$$

It then follows that

$$u_\alpha = u_\alpha^P + O(a) \quad \text{and} \quad a u_3 = a u_3^P + O(a) \quad \text{in } \Omega \tag{7}$$

where $O(a)$ is any vanishing quantity when a vanishes and u^P satisfies the Love–Kirchhoff kinematic relations

$$\partial_3 u_3^P = 0, \qquad u_\alpha^P = \overline{u}_\alpha^P - x_3 \partial_{x_\alpha} u_3^P \quad \text{with } \partial_3 \overline{u}_\alpha^P = 0 \text{ for } \alpha = 1, 2 \text{ in } \Omega_E.$$

Please cite this article in press as: M. Lenczner, R.C. Smith, A two-scale model for an array of AFM's cantilever in the static case, Mathematical and Computer Modelling (2007), doi:10.1016/j.mcm.2006.12.028

In this paper, we neglect the contribution of the membrane displacement $\overline{u}^P$ so we state only the model satisfied by the transverse displacement u_3^P. It is governed by the equilibrium equations, the stress–strain relations and the rigidity constraint

$$\operatorname{div}(\operatorname{div}(M^P)) = f^P + \operatorname{div}(g^P), \quad M^P = R^P \nabla\nabla^{\mathrm{T}} u_3^P \text{ in } \omega_E \text{ and } u_3^P = b^P + B_1^P x_1 + B_2^P x_2 \text{ in } \omega_R \tag{8}$$

where

$$g_\alpha^P(x_1, x_2) = \int_{-a}^{a} f_\alpha(x) x_3 \mathrm{d}x_3 \quad \text{and} \quad f^P(x_1, x_2) = \int_{-a}^{a} f_3(x)\mathrm{d}x_3 \quad \text{in } \omega_E. \tag{9}$$

In the case of isotropic materials, the elasticity can be formulated as

$$R^P_{\alpha\beta\gamma\rho} = a^3 \left(\frac{4\lambda\mu}{3(\lambda + 2\mu)} \delta_{\alpha\beta}\delta_{\gamma\rho} + \frac{4\mu}{3}\delta_{\alpha\gamma}\delta_{\beta\rho} \right). \tag{10}$$

In addition, $x = (x_1, x_2)^{\mathrm{T}}$, b^P is a scalar and B^P is a two-dimensional vector.

The boundary conditions are

$$\begin{aligned} &u_3^P = \nabla u_3^P.n = 0 \quad \text{on } \gamma_0^P \\ &\text{and} \quad n^{\mathrm{T}} M^P n = 0, \qquad \nabla(n^{\mathrm{T}} M^P \tau).\tau + \operatorname{div}(M^P).n = g^P.n \quad \text{on } \gamma_1^P \end{aligned} \tag{11}$$

where n and τ are the unit outward normal and the unit tangent to the boundary of ω_E. The transmission condition at the interface $\gamma_{E,R}$ results from the continuity conditions of the displacement u_3^P and of its gradient ∇u_3^P and the continuity of the normal stresses. These can be expressed as

$$\begin{aligned} &b^P = |\gamma_{E,R}|^{-1} \int_{\gamma_{E,R}} (u_3^P - \nabla u_3^P.x)_{|\omega_E} \mathrm{d}s, \qquad B^P = |\gamma_{E,R}|^{-1} \int_{\gamma_{E,R}} (\nabla u_3^P)_{|\omega_E} \mathrm{d}s \\ &\quad - \int_{\gamma_{E,R}} \operatorname{div}(M^P).n \mathrm{d}s = \xi^P \quad \text{and} \quad \int_{\gamma_{E,R}} (n^{\mathrm{T}} M^P)_\alpha - (\operatorname{div}(M^P).n) x_\alpha \mathrm{d}s = \Xi_\alpha^P \end{aligned} \tag{12}$$

where

$$\xi^P = -\int_{\gamma_{E,R}} (g^P.n)_{|\omega_E} \mathrm{d}s + \int_{\omega_R} f^P \mathrm{d}x, \qquad \Xi_\alpha^P = -\int_{\gamma_{E,R}} (g^P.n)_{|\omega_E} x_\alpha \mathrm{d}s + \int_{\omega_R} f^P x_\alpha - g_\alpha^P \mathrm{d}x,$$

$|\gamma_{E,R}|$ denotes the length of the interface $\gamma_{E,R}$, g^P and f^P have been defined in ω_E and are defined in ω_R by

$$g_\alpha^P(x_1, x_2) = \int_{-h(x_1,x_2)}^{a} f_\alpha(x) x_3 \mathrm{d}x_3 \quad \text{and} \quad f^P(x_1, x_2) = \int_{-h(x_1,x_2)}^{a} f_3(x)\mathrm{d}x_3 \quad \text{in } \omega_R.$$

The variational formulation associated with this model is

$$u_3^P \in V^P \quad \text{and} \quad \int_{\omega_E} M^P :: \nabla\nabla^{\mathrm{T}} v \mathrm{d}x = \int_{\omega_P} f^P v - g^P.\nabla v \mathrm{d}x \quad \text{for all } v \in V^P \tag{13}$$

taking into account the stress–strain relation. The set of admissible transverse displacements is

$$V^P = \{v \in H^2(\omega_P) / \nabla\nabla^{\mathrm{T}} v = 0 \text{ in } \omega_R \text{ and } v = \nabla v.n = 0 \text{ on } \gamma_0^P\}$$

with $H^2(\omega_P)$ being the set of square integrable functions on ω_P so that their first-order and second-order derivatives are also square integrable.

Remark 1. For the derivation of the two-scale model, we need an extension of this model for plates with varying thickness, namely, when Ω_E and Ω_R are replaced by

$$\begin{aligned} &\Omega_E = \{x \in \mathbb{R}^3 / (x_1, x_2) \in \omega_E \text{ and } -k(x_1, x_2) < x_3 < k(x_1, x_2)\} \\ &\Omega_R = \{x \in \mathbb{R}^3 / (x_1, x_2) \in \omega_R \text{ with } -h(x_1, x_2) < x_3 < k(x_1, x_2)\} \end{aligned}$$

where k is a positive function so that $a^{-1}k = O(1)$. In such a case, the model remains the same except that a is replaced by k in the expressions of the two-dimensional forces (9) and of the two-dimensional rigidities (10).

Please cite this article in press as: M. Lenczner, R.C. Smith, A two-scale model for an array of AFM's cantilever in the static case, Mathematical and Computer Modelling (2007), doi:10.1016/j.mcm.2006.12.028

3.2. Justification of the thin plate model

The justification of the thin plate model is based on the asymptotic method of Ciarlet [2] and of Destuynder [1]. In these works, the thin plate model is derived for isotropic elastic bodies by calculating the asymptotic behavior of the elasticity system and of its solution when the parameter a vanishes. In this work we use the same method but our derivation is based on the paper by Canon and Lenczner [6] where material anisotropy was encompassed. The only difference between the new model and that in [6] comes from the presence of the rigid body which does not significantly affect the proofs. Hence we report only the main steps in the calculations.

Since the asymptotic method consist of finding the limit when a vanishes, it is mandatory to introduce a scaled domain independent of a and to formulate the problem on it. To do so, one introduces the change of variable F^a defined on Ω by $F^a(x) = (x_1, x_2, \frac{1}{a}x_3)$ in Ω. The image $F^a(\Omega)$ is denoted by $\widetilde{\Omega}$ and there the coordinates are $\widetilde{x} = F^a(x)$. The whole model is now expressed on the dilated domain. All variables or fields related to $\widetilde{\Omega}$ are covered by a tilde. The rigidity, the mechanical displacement and the forces are scaled in different manners:

$$\widetilde{R}(\widetilde{x}) = R(x), \qquad \widetilde{u}(\widetilde{x}) = (u_1, u_2, au_3)(x), \qquad \widetilde{f}(\widetilde{x}) = \left(f_1, f_2, \frac{1}{a} f_3\right)(x) \quad \text{for } x \in \Omega.$$

From the assumption made on f, it is clear that $\|\widetilde{f}\|_{\widetilde{\Omega}}$ is bounded. We also apply a scaling to the test functions

$$\widetilde{v}(\widetilde{x}) = (v_1, v_2, av_3)(x).$$

For a given displacement field v, define the 3×3 matrix $K(\widetilde{v})$ such that $K_{\alpha\beta}(\widetilde{v}) = s_{\alpha\beta}(\widetilde{v})$, $K_{\alpha 3}(\widetilde{v}) = K_{3\alpha}(\widetilde{v}) = a^{-1}s_{3\alpha}(\widetilde{v})$ and $K_{33}(\widetilde{v}) = a^{-2}s_{33}(\widetilde{v})$. Applying the variable change $\widetilde{x} = F^a(x)$ in (3) yields the following variational formulation: find $\widetilde{u} \in \widetilde{V}$ such that

$$a \int_{\widetilde{\Omega}_E} \widetilde{\sigma} :: K(\widetilde{v}) \mathrm{d}\widetilde{x} = a \int_{\widetilde{\Omega}} \widetilde{f}(\widetilde{x}).\widetilde{v}(\widetilde{x}) \mathrm{d}\widetilde{x} \tag{14}$$

for all $\widetilde{v} \in \widetilde{V}$, where $\widetilde{\sigma} = \widetilde{R} K(\widetilde{u})$ and

$$\widetilde{V} = \{\widetilde{v} \in H^1(\widetilde{\Omega})^3 / K(\widetilde{v}) = 0 \text{ in } \widetilde{\Omega}_R \text{ and } \widetilde{v} = 0 \text{ on } \widetilde{\Gamma}_0\}.$$

By equating $\widetilde{v} = \widetilde{u}$, one may prove that $\|\widetilde{u}\|_{\widetilde{\Omega}}$ and $\|K(\widetilde{u})\|_{\widetilde{\Omega}}$ are $O(1)$ with respect to a. Thus we are led to formulate

$$\widetilde{u} = \widetilde{u}^P + O(a), \qquad K(\widetilde{u}) = K^P + O(a)$$

where $\widetilde{u}^P$ and K^P are independent of a. It follows that

$$K^P_{\alpha\beta} = s_{\alpha\beta}(\widetilde{u}^P) \quad \text{for } \alpha, \beta = 1, 2 \quad \text{and that} \quad s_{i3}(\widetilde{u}^P) = 0 \quad \text{for } i = 1, 2, 3.$$

This is equivalent to saying that $\widetilde{u}^P$ fulfills the Love–Kirchhoff kinematics

$$\partial_{\widetilde{x}_3} \widetilde{u}^P_3 = 0 \quad \text{and} \quad \widetilde{u}^P_\alpha = \widetilde{\widetilde{u}}^P_\alpha - \widetilde{x}_3 \partial_{x_\alpha} \widetilde{u}^P_3 \quad \text{with } \partial_{\widetilde{x}_3} \widetilde{\widetilde{u}}^P_\alpha = 0.$$

When neglecting the membrane displacement $\widetilde{\widetilde{u}}_\alpha$, it appears that $\widetilde{u}^P_3$ solves the variational formulation, which is independent of the parameter a,

$$\widetilde{u}^P_3 \in V^P, \quad \int_{\omega_E} \widetilde{M}^P :: \nabla\nabla^{\mathrm{T}} \widetilde{v}_3 \mathrm{d}\widetilde{x} = \int_{\widetilde{\Omega}} \widetilde{f}_3 \widetilde{v}_3 - \widetilde{x}_3 \widetilde{f}_\alpha \partial_{\widetilde{x}_\alpha} \widetilde{v}_3 \mathrm{d}\widetilde{x} \quad \text{for all } \widetilde{v}_3 \in V^P.$$

Here $\widetilde{M}^P = \widetilde{R}^P \nabla\nabla^{\mathrm{T}} \widetilde{u}^P_3$ and $\widetilde{R}^P$ is defined under the name Q^{22} in Canon and Lenczner [6] and is equal to

$$\widetilde{R}^P_{\alpha\beta\gamma\rho} = \frac{4\lambda\mu}{3(\lambda + 2\mu)} \delta_{\alpha\beta}\delta_{\gamma\delta} + \frac{4\mu}{3} \delta_{\alpha\gamma}\delta_{\beta\rho}$$

in the case of an isotropic material. Applying the inverse variable change, u^P_3 solves the variational formulation: find $u^P_3 \in V^P$ such that

$$\int_{\omega_E} M^P :: \nabla\nabla^{\mathrm{T}} v_3 \mathrm{d}x = \int_{\Omega} (f_3 v_3 - x_3 f_\alpha \partial_{x_\alpha} v_3) \mathrm{d}x$$

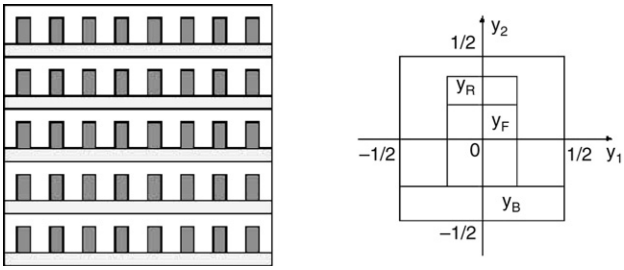

Fig. 2. Array of cantilevers and their reference cell.

for all $v_3 \in V^P$ with $M^P = R^P \nabla\nabla^T u_3^P$ and $R^P = a^3 \widetilde{R}^P$. This leads directly to the variational formulation (13). Since $\nabla\nabla^T v_3 = 0$ in Ω_R it may be written as $v_3 = d + D.x$ with $D = (D_1, D_2)^T$; thus the right-hand side may be reformulated as

$$\int_{\omega_E} (f^P v_3 - g^P.\nabla v_3)\mathrm{d}x + \xi^P d^P + \Xi^P.D^P.$$

On application of the Green formula twice, and using the fact that $v_3 = d + D.x$ on $\gamma_{E,R}$, it follows that

$$\int_{\omega_E} \mathrm{div}(\mathrm{div}(M^P)v_3)\mathrm{d}x + \int_{\gamma_1} (n^T M^P \nabla v_3 - \mathrm{div}(M^P).n v_3)\mathrm{d}s$$
$$- \left(\int_{\gamma_{E,R}} \mathrm{div}(M^P).n\mathrm{d}s\right) d^P + \left(\int_{\gamma_{E,R}} (n^T M^P - \mathrm{div}(M^P).nx)\mathrm{d}s\right).D^P$$
$$= \int_{\omega_E} (f_3^P + \mathrm{div}(g^P))v_3\mathrm{d}x - \int_{\gamma_1} g^P.n v_3 \mathrm{d}s + \xi^P d^P + \Xi^P.D^P$$

from which we deduce all the model equations except the continuity condition of u_3^P and ∇u_3^P that comes by integrating the expressions $u_3^P = b^P + B^P.x$ and $\nabla u_3^P = B^P$ on $\gamma_{E,R}$.

4. Model for an AFM array

Consider a mechanical structure made of a periodic distribution of microcantilevers as shown on Fig. 2. In Section 4.1 a simplified model is stated when its derivation is done in Section 4.2.

4.1. Statement of the model

The whole domain occupied by the cantilever array is still denoted by ω_P and is assumed to be embedded in the macroscopic domain $\omega = (0, L_1) \times (0, L_2)$. It is constituted of $n_1 \times n_2$ square cells Y_i^ε of size $\varepsilon \times \varepsilon$ and fills up ω, so $L_1 = n_1\varepsilon$ and $L_2 = n_2\varepsilon$. The cells are indexed with multi-indices $i = (i_1, i_2)$ varying from 1 to n_1 and from 1 to n_2.

The dilatation and shift of any cell Y_i^ε give rise to a reference unit cell $Y \subset (-\frac{1}{2}, \frac{1}{2})^2$. For the derivation of the array model, we assume that $\varepsilon/L_1 << 1$. As ω_P, this microscopic cell is comprised of a thin elastic plate Y_E and a rigid part Y_R. In Y_E, we distinguish the base Y_B and the elastic part of the cantilever Y_F that is assumed to be much more flexible than the base. The entire cantilever, made up of Y_F and of the rigid part Y_R, is denoted by Y_C. In ω, the bases and the cantilevers are respectively denoted by ω_B and ω_C.

Consider a function v defined on ω. Its two-scale transform $\widehat{v}(x, y)$ is the function defined on $\omega \times Y$ by

$$\widehat{v}(x, y) = \sum_i \chi_{Y_i^\varepsilon}(x) v(x_i^\varepsilon + \varepsilon y) \tag{15}$$

where the sum holds for all the cells $Y_i^\varepsilon \subset \omega$, x_i^ε are the centers of those cells and $\chi_{Y_i^\varepsilon}$ is the characteristic function of Y_i^ε. The two-scale transform of a function v defined in ω_P only is accomplished through the same definition but after having extended v by zero to ω. The assumptions as well as the model are stated on the two-scale transforms of the various fields playing a role. We quantify the fact that Y_F is much more supple than the base by saying that both

$$\varepsilon^{-4}\widehat{R}^P = R^C + O(\varepsilon) \quad \text{in } Y_F \quad \text{and} \quad \widehat{R}^P = R^B + O(\varepsilon) \quad \text{in } Y_B$$

with R^C and R^B independent of ε. In other words, we consider that the plate has a varying thickness which is equal to $2a_B$ in Y_B and $2a_C$ in Y_C with the ratio $a_C^3/a_B^3 \sim \varepsilon^4$. The thin plate model with varying thickness has been discussed in Remark 1. In addition, we are led to assume that

$$\widehat{f}^P = f^0 + O(\varepsilon) \quad \text{in } Y, \qquad \widehat{g}^P = g^B + O(\varepsilon) \quad \text{in } Y_B \quad \text{and} \quad \varepsilon^{-1}\widehat{g}^P = g^C + O(\varepsilon) \quad \text{in } Y_C$$

with f^0, g^B and g^C independent of ε. Based on these assumptions in ω_B, it follows that

$$u_3^P = \overline{u^M} + O(\varepsilon), \qquad \nabla u_3^P = \overline{D(u^M,\theta)} + O(\varepsilon)$$
$$\text{and} \quad \nabla\nabla^{\mathrm{T}} u_3^P = \overline{D^2(u^M,\theta)} + \overline{\mathcal{L}^B D^2(u^M,\theta)} + O(\varepsilon) \tag{16}$$

whereas in ω_C, it follows that

$$u_3^P = \overline{u^M} + \overline{u^C} + O(\varepsilon),$$
$$\varepsilon\nabla u_3^P = \overline{\nabla_y u^C} + O(\varepsilon) \quad \text{and} \quad \varepsilon^2\nabla\nabla^{\mathrm{T}} u_3^P = \overline{\nabla_y\nabla_y^{\mathrm{T}} u^C} + O(\varepsilon) \tag{17}$$

where ∇_y is the gradient with respect to y,

$$D(u^M,\theta) = \begin{pmatrix} \partial_{x_1} u^M \\ \theta \end{pmatrix} \quad \text{and} \quad D^2(u^M,\theta) = \begin{pmatrix} \partial^2_{x_1x_1} u^M & \partial_{x_1}\theta \\ \partial_{x_1}\theta & 0 \end{pmatrix}$$

and $\overline{v}$ is defined on ω_P by

$$\overline{v}(x) = \frac{1}{\varepsilon}\int_{(i_2-1)\varepsilon}^{i_2\varepsilon} v\left(x_1, z, \frac{x}{\varepsilon} - \frac{1}{2}\right)\mathrm{d}z \quad \text{for all } x \in Y_i^\varepsilon \text{ and } i = (i_1, i_2)$$

after $y \mapsto v(x,y)$ has been extended by Y-periodicity to $\mathbb{R}^2$.

The construction of (u^M,θ), of the fourth-order tensor $\mathcal{L}^B$ and of u^C is done as follows. First, one builds $\mathcal{L}^B$ so that

$$(\nabla_y\nabla_y^{\mathrm{T}} w^B)_{\alpha\beta} = \sum_{\gamma,\rho=1}^{2} \mathcal{L}^B_{\alpha\beta\gamma\rho}\begin{pmatrix} \nu & \mu \\ \mu & 0 \end{pmatrix}_{\gamma\rho} \tag{18}$$

where w^B is solution of the microscopic Problem $\mathcal{P}_B$ posed in the base Y_B. Once this is done, the calculation of (u^M,θ) is made possible by solving the Problem macro $\mathcal{P}^M$ related to the macroscopic domain ω and the base Y_B. Finally, u^M being known, u^C may be computed due to the microscopic Problem $\mathcal{P}^C$ posed in Y_C. We note that in the case of atomic forces depending on u^C, the macroscopic Problem $\mathcal{P}^M$ and the microscopic Problem $\mathcal{P}^C$ in the cantilever cannot be solved sequentially since they are fully coupled through the expression of the atomic forces when its action on the tip has a non-negligible effect on the base's solution (u^M,θ).

Problem $\mathcal{P}^M$. The set of edges of the macroscopic domain ω where $x_1 = 0$ or 1 splits in γ_0^M and γ_1^M corresponding, respectively, to the area where the base is clamped and where it is free. The statement of the macroscopic or homogenized Problem $\mathcal{P}^M$ includes the equilibrium equations

$$\partial^2_{x_1x_1} M_1^M = f_1^M \quad \text{and} \quad \partial_{x_1} M_2^M = f_2^M \quad \text{in } \omega \tag{19}$$

and the stress–strain relation

$$M_1^M = R_{11}^M \partial^2_{x_1x_1} u^M + R_{12}^M \partial_{x_1}\theta, \qquad M_2^M = R_{21}^M \partial^2_{x_1x_1} u^M + R_{22}^M \partial_{x_1}\theta \quad \text{in } \omega \tag{20}$$

along with the boundary conditions

$$u^M = \partial_{x_1} u^M = \theta = 0 \quad \text{on } \gamma_0^M$$
$$\text{and} \quad M_1^M = M_2^M = 0, \qquad \partial_{x_1} M_1^M = g^M \quad \text{on } \gamma_1^M. \tag{21}$$

Please cite this article in press as: M. Lenczner, R.C. Smith, A two-scale model for an array of AFM's cantilever in the static case, Mathematical and Computer Modelling (2007), doi:10.1016/j.mcm.2006.12.028

The new parameters are

$$g^M = \int_{Y_B} g_1^B \mathrm{d}y, \qquad f_1^M = \int_Y f^0 \mathrm{d}y + \int_{Y_B} \partial_{x_1} g_1^B \mathrm{d}y, \qquad f_2^M = \int_{Y_B} g_2^B \mathrm{d}y$$

$$R^M = \begin{pmatrix} \widetilde{R}^M_{1111} & 2\widetilde{R}^M_{1211} \\ 2\widetilde{R}^M_{1211} & 4\widetilde{R}^M_{1212} \end{pmatrix}$$

where the fourth-order tensor $\widetilde{R}^M$ is defined by

$$\widetilde{R}^M_{\alpha\beta\gamma\rho} = \int_{Y_B} R^B_{\alpha\beta\gamma\rho} + R^B_{\alpha\beta\xi\zeta} \mathcal{L}^B_{\xi\zeta\gamma\rho} \mathrm{d}y,$$

$\mathcal{L}^B$ is defined by (18) and w^B is solution of Problem $\mathcal{P}^B$.

The variational formulation is

$$(u^M, \theta) \in V^M, \quad \int_\omega M^M.(\partial^2_{x_1 x_1} v, \partial_{x_1} \eta)^{\mathrm{T}} \mathrm{d}x = \int_\omega f_1^M v - g^M.D(v, \eta) \mathrm{d}x \quad \text{for all } (v, \eta) \in V^M \tag{22}$$

where

$$V^M = \{(v, \eta) \in L^2(\omega)^2 / \partial^2_{x_1 x_1} v \text{ and } \partial_{x_1} \theta \in L^2(\omega), v = \partial_{x_1} v = \theta = 0 \text{ on } \gamma_0^M\},$$

$L^2(\omega)$ being the set of square integrable functions on ω.

Problem $\mathcal{P}^B$. The boundary of Y_B is made up of the interface $\gamma_{B,F}$ between Y_B and Y_F, the area γ_{per} corresponding to the junction between neighboring cells and the remaining part γ_{B1}. The microscopic equations stated in the base Y_B are

$$\mathrm{div}_y(\mathrm{div}_y(M^B)) = -\mathrm{div}_y(\mathrm{div}_y(F^B)) \quad \text{with } M^B = R^B \nabla_y \nabla_y^{\mathrm{T}} w^B \text{ and } F^B = R^B \begin{pmatrix} \nu & \alpha \\ \alpha & 0 \end{pmatrix}. \tag{23}$$

The boundary conditions are

$$\begin{aligned} &\nabla_y(n_y^{\mathrm{T}} M^B \tau_y).\tau_y + \mathrm{div}_y(M^B).n_y = -\nabla_y(n_y^{\mathrm{T}} F^B \tau_y).\tau_y - \mathrm{div}_y(F^B).n_y \\ &\text{and} \quad n_y^{\mathrm{T}} M^B n_y = -n_y^{\mathrm{T}} F^B n_y \quad \text{on } \gamma_{B1} \cup \gamma_{B,F} \end{aligned}$$

and

$$w^B, \qquad n_y^{\mathrm{T}} M^B n_y, \qquad \nabla w^B.n, \qquad \nabla_y(n_y^{\mathrm{T}} M^B \tau_y).\tau_y + \mathrm{div}_y(M^B).n_y \quad \text{are } Y\text{-periodic on } \gamma_{\mathrm{per}}.$$

The variational formulation is

$$u^B \in V^B, \quad \int_{Y_B} M^B :: \nabla_y \nabla_y^{\mathrm{T}} v \mathrm{d}y = -\int_{Y_B} F^B \nabla_y \nabla_y^{\mathrm{T}} v \mathrm{d}x \quad \text{for all } v \in V^B \tag{24}$$

where

$$V^B = \{v \in H^2(Y_B)/v, \nabla_y v \text{ are } Y\text{- periodic on } \gamma_{\mathrm{per}}\}.$$

We note that the solution of this variational formulation is unique up to a function v such that $\nabla_y \nabla_y^{\mathrm{T}} v = 0$ and v, $\nabla_y v$ are Y-periodic on γ_{per}, in short up to a function $v(y) = a_0 + a_1 y_2$.

Problem $\mathcal{P}^C$. The boundary of the elastic part Y_F of the cantilever is the union of the interface $\gamma_{B,F}$ between the base and the cantilever, the interface $\gamma_{B,R}$ between the elastic part and the rigid part and the remaining γ_{F1}. The data $\widehat{f^P}$ and g^C being given, the Problem $\mathcal{P}^C$ used for the calculation of u^C is made up of the equilibrium equations, the stress–strain relation and the rigidity constraint

$$\mathrm{div}_y(\mathrm{div}_y(M^C)) = f^0 + \mathrm{div}_y g^C \quad \text{and} \quad M^C = R^C \nabla_y \nabla_y^{\mathrm{T}} u^C \quad \text{in } Y_F, \tag{25}$$

$$u^C = b^C + B^C.y \quad \text{in } Y_R,$$

the boundary conditions

$$u^C = \nabla_y u^C.n_y = 0 \quad \text{on } \gamma_{B,F},$$
$$n_y^{\mathrm{T}} M^C n_y = 0, \qquad \nabla_y(n_y^{\mathrm{T}} M^C \tau_y).\tau_y + \mathrm{div}_y(M^C).n_y = 0 \quad \text{on } \gamma_{F1},$$

the continuity of u^C and $\nabla_y u^C$ through the interface $\gamma_{F,R}$ and the normal stresses transmission

$$b^C = |\gamma_{F,R}|^{-1} \int_{\gamma_{F,R}} (u^C - \nabla_y u^C.y)_{|Y_F} \mathrm{d}s, \qquad B^C = |\gamma_{F,R}|^{-1} \int_{\gamma_{F,R}} (\nabla_y u^C)_{|Y_F} \mathrm{d}s$$
$$- \int_{\gamma_{F,R}} \mathrm{div}_y(M^C).n_y \mathrm{d}s = \xi^C, \qquad \int_{\gamma_{F,R}} n_y^{\mathrm{T}} M^C - (\mathrm{div}_y(M^C).n_y) y \mathrm{d}s = \Xi^C$$

where

$$\xi^C = \int_{Y_R} f^0 \mathrm{d}y - \int_{\gamma_{F,R}} (g^C.n_y)_{|Y_F} \mathrm{d}s \quad \text{and} \quad \Xi^C = \int_{\gamma_{F,R}} -(g^C.n_y)_{|Y_F} y \mathrm{d}s + \int_{Y_R} f^0 y - g^C \mathrm{d}y. \tag{26}$$

The corresponding variational formulation is

$$u^C \in V^C, \quad \int_{Y_F} M^C :: \nabla_y \nabla_y^{\mathrm{T}} v \mathrm{d}y = \int_{Y_C} f^0 v - g^C.\nabla_y v \mathrm{d}y \quad \text{for all } v \in V^C \tag{27}$$

where

$$V^C = \{v \in H^2(Y_C) / v = \nabla_y v.n_y = 0 \text{ on } \gamma_{B,F},\ \nabla_y \nabla_y^{\mathrm{T}} v = 0 \text{ in } Y_R\}.$$

4.2. *Derivation of the two-scale model*

The proof follows three steps. First a specific estimate of the growth of the mechanical displacement is derived with respect to the small parameter ε. In a second step we use the Taylor expansion of the two-scale transform of u_3^P and identify the global system which is verified by the coefficients of the Taylor expansion. It is from this global system that the wanted model is extracted.

The mathematical formulation of the assumptions on the rigidity and on the external forces is on the one side a uniform ellipticity condition: there exists a constant K such that for all $\varepsilon > 0$ and all 2×2 symmetric matrix ξ,

$$[R^B \xi] :: \xi \quad \text{and} \quad [R^C \xi] :: \xi \geq K |\xi|^2$$

and on the other side there exists another constant C such that, for all $\varepsilon > 0$,

$$\|\widehat{f}^P\|_{\omega \times Y} + \|\widehat{g}^P\|_{\omega \times Y_B} + \|\varepsilon^{-1} \widehat{g}^P\|_{\omega \times Y_C} \leq C.$$

Relaxed variational formulation: The derivation of the model satisfied by (u^M, θ, u^B, u^C) is easier to do on a variational formulation where the constraint of rigidity and the boundary conditions have been removed from the set of admissible fields: Find $u_3^P \in H^2(\omega_P)$ and $\lambda^P \in N^P$ such that

$$a^P(u_3^P, v) + d^P(\lambda^P, v) = l^P(v) \quad \text{and} \quad d^P(\mu^P, u_3^P) = 0 \quad \text{for all } v \in H^2(\omega_P) \text{ and } \mu^P \in N^P \tag{28}$$

where

$$a^P(u_3^P, v) = \int_{\omega_P} M^P :: \nabla \nabla^{\mathrm{T}} v \mathrm{d}x, \, l^P(v) = \int_{\omega_P} f^P v - g^P.\nabla v \mathrm{d}x$$
$$d^P(\lambda^P, v) = \int_{\omega_R} \lambda^{P,R} :: \nabla \nabla^{\mathrm{T}} v \mathrm{d}x + \left\langle \lambda^{P,D}, (v, \partial_{x_1} v, \partial_{x_2} v)^{\mathrm{T}} \right\rangle_{\gamma_0^P}$$

and $N^P = \{\lambda^P = (\lambda^{P,R}, \lambda_1^{P,D}, \lambda_2^{P,D}, \lambda_3^{P,D}) \in L_S^2(\omega_R)^4 \times (H^{3/2}(\gamma_0^P))' \times (H^{1/2}(\gamma_0^P)^2)'\}$, $L_S^2(\omega_R)^4$ being the set of 2×2 symmetric matrices with coefficients in $L^2(\omega_R)$.

Please cite this article in press as: M. Lenczner, R.C. Smith, A two-scale model for an array of AFM's cantilever in the static case, Mathematical and Computer Modelling (2007), doi:10.1016/j.mcm.2006.12.028

Estimates: The following norms

$$\|u_3^P\|_{\omega_P},\quad \|\nabla u_3^P\|_{\omega_B},\quad \|\varepsilon\nabla u_3^P\|_{\omega_C},\quad \|\nabla\nabla^{\mathrm{T}}u_3^P\|_{\omega_B},\quad \|\varepsilon^2\nabla\nabla^{\mathrm{T}}u_3^P\|_{\omega_C},\quad \|\varepsilon^{-2}\lambda^{P,R}\|_{\omega_R},\tag{29}$$
$$\|\lambda_1^{P,D}\|_{H^{3/2}(\gamma_0^P)'}\quad\text{and}\quad \|\lambda_2^{P,D},\lambda_3^{P,D}\|_{(H^{1/2}(\gamma_0^P)')^2}\le C$$

uniformly with respect to ε. We only sketch the proof of this classical result. For the sake of simplicity, we remove the superscript of u_3^P, f^P and g^P in that proof. One starts from the variational formulation (28) where one equals $v=u$

$$\int_{\omega_B}[R^P\nabla\nabla^{\mathrm{T}}u]::\nabla\nabla^{\mathrm{T}}u\mathrm{d}x+\int_{\omega_C}\varepsilon^{-4}[R^P(\varepsilon^2\nabla\nabla^{\mathrm{T}}u)]::(\varepsilon^2\nabla\nabla^{\mathrm{T}}u)\mathrm{d}x=l^P(u),$$

one applies the uniform ellipticity condition and uses the fact that $\nabla\nabla^{\mathrm{T}}u=0$ in ω_R,

$$X=K(\|\nabla\nabla^{\mathrm{T}}u\|_{\omega_B}^2+\|\varepsilon^2\nabla\nabla^{\mathrm{T}}u\|_{\omega_C}^2)\le\|f\|_{\omega_P}\|u\|_{\omega_P}+\|(\chi_{\omega_B}+\varepsilon^{-1}\chi_{\omega_C})g\|_{\omega_P}\|(\chi_{\omega_B}+\varepsilon\chi_{\omega_C})\nabla u\|_{\omega_P},$$

and then the estimates on the external forces

$$X\le C_1(\|u\|_{\omega_P}+\|(\chi_{\omega_B}+\varepsilon\chi_{\omega_C})\nabla u\|_{\omega_P}).$$

Thanks to the Poincaré-like estimate (82),

$$X\le C_2\|(\chi_{\omega_B}+\varepsilon^2\chi_{\omega_C})\nabla\nabla^{\mathrm{T}}u\|_{\omega_P}.$$

The conclusion follows.

Approximation of the two-scale transforms: We assume that u_3^P can be expanded as $\widehat{u}_3^P=u^0+\varepsilon\widetilde{u}^1+\varepsilon^2\widetilde{u}^2+\varepsilon^2O(\varepsilon)$ in $\omega\times Y_B$ which is partially justified by (29). Let us apply the results of the Appendix A.4 to u_3^P on $\omega_1=\omega_B$ and let us introduce the notations

$$u^M=u^0_{|\omega\times Y_B},\qquad \theta=\partial_{y_2}u^1\quad\text{and}\quad u^B=u^2\quad\text{in }\omega\times Y_B.$$

Then,

$$\widehat{u}_3^P=u^M+O(\varepsilon),\qquad \widehat{\nabla u_3^P}=D(u^M,\theta)+O(\varepsilon)$$
$$\text{and}\quad \widehat{\nabla\nabla^{\mathrm{T}}u_3^P}=D^2(u^M,\theta)+\nabla_y\nabla_y^{\mathrm{T}}u^B+O(\varepsilon)\quad\text{in }\omega\times Y_B\tag{30}$$

in the weak sense, with

$$(u^M,\theta)\in V^M,u^B\in V^B,u^C\in L^2(\omega;H^2(Y_C))\text{ and }u^C=\nabla u^C.n_y=0\quad\text{on }\omega\times\gamma_{B,F}.\tag{31}$$

Now let us assume that $\widehat{u}_3^P=u^0+O(\varepsilon)$ in $\omega\times Y_C$ and let us apply the results of subsection Appendix A.4 applied to u_3^P on $\omega_1=\omega_C$; then

$$\widehat{u}_3^P=u^M+u^C+O(\varepsilon),\qquad \varepsilon\widehat{\nabla u_3^P}=\nabla_y u^C+O(\varepsilon),$$
$$\varepsilon^2\widehat{\nabla\nabla^{\mathrm{T}}u_3^P}=\nabla_y\nabla_y^{\mathrm{T}}u^C+O(\varepsilon)\quad\text{in }\omega\times Y_C\tag{32}$$

in the weak sense, where $u^C=u^0-u^M$ and with

$$u^C,\qquad \nabla_y u^C\quad\text{and}\quad\nabla_y\nabla_y^{\mathrm{T}}u^C\quad\text{in }L^2(\omega\times Y_C).\tag{33}$$

The approximations (16) and (17) come from (30) and (32) combined with (35) and with (70). In the following we establish the model satisfied by (u^M,θ,u^C,u^B). Let us introduce the space of admissible fields,

$$V^A=\{(u^M,\theta,u^C,u^B)/(31)\text{ and }(33)\}.$$

Concerning the Lagrange multipliers, from (29) we postulate that

$$\varepsilon^{-2}\widehat{\lambda^{P,R}}=\lambda^{A,R}+O(\varepsilon)\quad\text{and}\quad\widehat{\lambda^{P,D}}=\lambda^{A,D}+O(\varepsilon)\tag{34}$$

with $\lambda^A = (\lambda^{A,R}, \lambda_1^{A,D}, \lambda_2^{A,D}, \lambda_3^{A,D}) \in N^A = L_S^2(\omega \times Y_R)^4 \times (H^{3/2}(\gamma_0^M))' \times (H^{1/2}(\gamma_0^M)^2)'$. We voluntarily prefer to skip the detailed mathematical argumentation on that point.

Test functions: Consider $(v^M, \eta, v^B, v^C, \mu^A) \in V^A \times N^A$, v^1 independent of y_1 constructed from η through $\partial_{y_2} v^1 = \eta$,

$$v = v^M + \varepsilon v^1 + \varepsilon^2 v^B \quad \text{in } \omega \times Y_B \quad \text{and} \quad v = v^M + v^C + O(\varepsilon) \quad \text{in } \omega \times Y_C$$

the term $O(\varepsilon)$ being so that $\overline{v} \in H^2(\omega_P)$. Such $(\overline{v}, \overline{\mu^A})$ may be chosen as a test functions in the variational formulation (28). From (73) and its reiteration

$$\nabla\nabla^{\mathrm{T}}\overline{v} = \overline{D^2(v^M, \eta)} + \overline{\nabla_y \nabla_y^{\mathrm{T}} v^B} + O(\varepsilon) \quad \text{in } \omega_B, \qquad \varepsilon^2 \nabla\nabla^{\mathrm{T}}\overline{v} = \overline{\nabla_y \nabla_y^{\mathrm{T}} v^C} + O(\varepsilon).$$

Approximation of the variational formulation: We choose $(\overline{v}, \overline{\mu^A})$ as test functions, apply the formulae (69) and then the approximations of the two-scale transforms (30), (32) and (34) to find

$$a^A((u^M, \theta, u^C, u^B), (v^M, \eta, v^B, v^C)) + d^A(\lambda^A, (v^M, \eta, v^C)) = l^A(v^M, \eta, v^C) + O(\varepsilon)$$
$$\text{and} \quad d^A(\mu^A, (u^M, \theta, u^C)) = O(\varepsilon)$$

for all $(v^M, \eta, v^B, v^C) \in V^A$ and $\mu^A \in N^A$ where

$$a^A((u^M, \theta, u^C, u^B), (v^M, \eta, v^B, v^C)) = \int_\omega \left[\int_{Y_B} M^B :: (D^2(v^M, \theta) + \nabla_y \nabla_y^{\mathrm{T}} v^B) \mathrm{d}y + \int_{Y_F} M^C :: \nabla_y \nabla_y^{\mathrm{T}} v^C \mathrm{d}y \right] \mathrm{d}x,$$

$$l^A(v^M, \eta, v^C) = \int_\omega \left[\int_{Y_B} f^0 v^M \mathrm{d}y + \int_{Y_C} f^0 (v^M + v^C) \mathrm{d}y - \int_{Y_B} g^B . D(v^M, \eta) \mathrm{d}y - \int_{Y_C} g^C . \nabla_y v^C \mathrm{d}y \right] \mathrm{d}x,$$

$$d^A(\lambda^A, (v^M, \eta, v^C)) = \int_{\omega \times Y_R} \lambda^{A,R} :: \nabla_y \nabla_y^{\mathrm{T}} v^C \mathrm{d}y \mathrm{d}x + \left\langle \lambda^{A,D}, (v^M, \partial_{x_1} v^M, \eta)^{\mathrm{T}} \right\rangle_{\gamma_0^M}$$

and $N^A = L_S^2(\omega \times Y_R)^4 \times (H^{3/2}(\gamma_0^M))' \times (H^{1/2}(\gamma_0^M)^2)'$.

In the following, we derive Problems $\mathcal{P}^B$, $\mathcal{P}^C$ and $\mathcal{P}^M$.

Derivation of $\mathcal{P}^B$: One starts by choosing $\eta = v^M = v^C = 0$ and remarking that

$$M = R^B D^2(u^M, \theta) + M^B;$$

then

$$\int_{\omega \times Y_B} M^B :: \nabla_y \nabla_y^{\mathrm{T}} v^B \mathrm{d}y \mathrm{d}x = \int_{\omega \times Y_B} -[R^B D^2(u^M, \theta)] :: \nabla_y \nabla_y^{\mathrm{T}} v^B \mathrm{d}y \mathrm{d}x.$$

Making the choice $v^B(x, y) = \varphi(x) \widetilde{v}^B(y)$ with any regular φ vanishing on the boundary of ω allows us to eliminate the integrals over ω and yields the variational formulation (23), where we have removed the $O(\varepsilon)$ term.

Derivation of $\mathcal{P}^C$: One poses $\eta = v^M = v^B = 0$ and $\nabla_y \nabla_y^{\mathrm{T}} v^C = 0$ in $\omega \times Y_R$ which leads to

$$\int_{\omega \times Y_F} M^C :: \nabla_y \nabla_y^{\mathrm{T}} v^C \mathrm{d}y \mathrm{d}x = \int_{\omega \times Y_C} f^0 . v^C - g^C . \nabla_y v^C \mathrm{d}y \mathrm{d}x.$$

Based on the same argument, the integrals over ω may be removed and (25) follows. The condition $\nabla_y \nabla_y^{\mathrm{T}} u^C = 0$ in $\omega \times Y_R$ comes directly from the second equation of the variational formulation.

Derivation of $\mathcal{P}^M$: Let us pose $v^B = v^C = 0$ and use the fact that

$$\nabla_y \nabla_y^{\mathrm{T}} u^B = \mathcal{L}^B D^2(u^M, \theta). \tag{35}$$

Please cite this article in press as: M. Lenczner, R.C. Smith, A two-scale model for an array of AFM's cantilever in the static case, Mathematical and Computer Modelling (2007), doi:10.1016/j.mcm.2006.12.028

It follows that

$$\int_{\omega} M^M :: D^2(v^M, \eta)\mathrm{d}y\mathrm{d}x = \int_{\omega\times Y_P} f^0.v^M \mathrm{d}y\mathrm{d}x - \int_{\omega\times Y_B} g^B.D(v^M, \eta)\mathrm{d}y\mathrm{d}x$$

and the variational formulation (22) follows.

5. Tip forces

To characterize the behavior of the cantilever, it is necessary to quantify the attractive forces F^{vdW} of van der Waals type and repulsive forces F^{rep} between the tip and sample. We consider first the development of relations for F^{vdW}.

As detailed in [21,28], attractive forces result primarily from van der Waals forces that are due to a combination of electrostatic and dispersional effects present between all atoms and molecules. Either classical or quantum principles can be used to derive the van der Waals potential

$$W^{vdW}(\zeta) = -\frac{C}{\|\zeta\|^6} \quad \text{where } \zeta = x' - x \tag{36}$$

for two atoms or molecules located respectively at the positions x and x'. Here $\|\zeta\| = (\zeta_1^2 + \zeta_2^2 + \zeta_3^2)^{1/2}$ and $C = \frac{\alpha_0^2 \hbar \nu}{(4\pi\varepsilon_0)^2}$ is a constant which depends on the electronic polarizability α_0 of constituent atoms, Planck's constant $\hbar$, the electron orbital frequency ν, and the permittivity ε_0 of vacuum.

To construct macroscopic relations quantifying the force between the cantilever tip and sample, we consider first the general case in which the tip and sample are arbitrary bodies Ω and Ω' having densities ρ and ρ'.

To determine the force, we make the classical assumptions of Hamaker which can be summarized as (i) additivity of individual atomic or molecular contributions, (ii) continuous media so that summation can be replaced by integration, and (iii) constant material properties. For these assumptions, the force exerted by the particle located in x' on this in x is given by

$$F^{vdW} = \rho\rho' \int_{\Omega}\int_{\Omega'} f(x' - x)\mathrm{d}x\mathrm{d}x' \tag{37}$$

where $f = -\nabla W^{vdW}$.

The determination of F for arbitrary geometries and potential W necessitates approximation of integrals over six dimensions, which is typically prohibitive. To simplify the formulation, we follow the approach of [26,27] and reformulate the relation in terms of surface integrals. We consider the vector field

$$G = \frac{-C\zeta}{3\|\zeta\|^6}. \tag{38}$$

It follows that

$$\operatorname{div} G = -W^{vdW} \tag{39}$$

and hence the divergence theorem can be invoked to formulate the macroscopic force as

$$F^{vdW} = \rho\rho' \int_{\partial\Omega}\int_{\partial\Omega'} (G.n')n\mathrm{d}s'\mathrm{d}s \tag{40}$$

where n and n' respectively denote normals to the tip and sample. For the vector field relation (38), the force is

$$F^{vdW} = -\frac{A}{3\pi^2} \int_{\partial\Omega}\int_{\partial\Omega'} \frac{\zeta.n'}{\|\zeta\|^6} n\mathrm{d}s'\mathrm{d}s \tag{41}$$

where the Hamaker constant is

$$A = \pi^2 C\rho\rho'. \tag{42}$$

Please cite this article in press as: M. Lenczner, R.C. Smith, A two-scale model for an array of AFM's cantilever in the static case, Mathematical and Computer Modelling (2007), doi:10.1016/j.mcm.2006.12.028

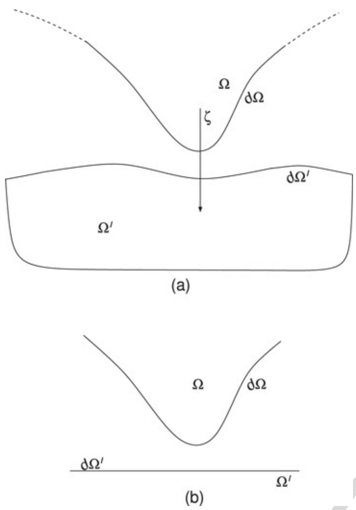

Fig. 3. Geometry of the AFM tip and sample with the assumption of (a) general surfaces, and (b) a locally flat sample.

The flat sample case: For various applications, it is reasonable to approximate the sample by a locally flat surface (n' constant) while retaining the general representation for the cantilever tip; see Fig. 3(b). For example, this assumption is reasonable when identifying the tip shape using a known sample with minimal curvature or for regimes in which the separation distance is large compared with perturbations in the sample. From the approximation

$$\int_{\partial\Omega'} \frac{\zeta.n'}{\|\zeta\|^6} n \mathrm{d}s' \approx \int_{\mathbb{R}^2} \frac{\zeta.n'}{\|\zeta\|^6} \mathrm{d}x_1' \mathrm{d}x_2' = \int_{\mathbb{R}^2} \frac{\zeta.n'}{\|\zeta\|^6} \mathrm{d}\zeta_1 \mathrm{d}\zeta_2 = \frac{\pi}{2(\zeta.n')^3}$$

the attractive force is

$$F^{v\mathrm{d}W} = \frac{A}{6\pi} \int_{\partial\Omega} \frac{n}{(\zeta.n')^3} \mathrm{d}s. \tag{43}$$

The simplified force relation (43) facilitates implementation when identifying the tip shape or operating in regimes in which the separation distance is sufficiently large so that modulations in the sample surface are negligible.

Flat sample and parameterized tip: Finally, we consider the case in which the sample surface is assumed locally flat and a simple geometric parameterization is assumed for the cantilever tip. Specifically, we follow the approach of Argento and French [26] and assume that the cantilever can be parameterized as having a spherical tip of radius R, and a conical section as depicted in Fig. 3 with a distance d from the sample. This geometry is motivated by scanning electron microscopy (SEM) images of various AFM tips and provides sufficient flexibility for a number of applications while limiting to commonly employed models for spherical probes.

This assumption allows cylindrical symmetry to be invoked to yield analytic force relations, and relaxation of this assumption would necessitate the approximation of nonsymmetric contributions which yield higher-order force effects.

As detailed in [26], the attractive force due to van der Waals interactions can in this case be expressed as

$$F^{v\mathrm{d}W}(d) = \frac{AR^2[1-\sin\gamma][R\sin\gamma - d\sin\gamma - R - d]}{6d^2[R+d-R\sin\gamma]^2} - \frac{A\tan\gamma[d\sin\gamma + R\sin\gamma + R\cos(2\gamma)]}{6\cos\gamma[d+R-R\sin\gamma]^2} \tag{44}$$

where A is the Hamaker constant specified in (42) and γ is the cone angle shown in Fig. 3.

The repulsive forces are due to the overlap of electron clouds. These are quantum mechanical in nature and very short range compared with the attractive forces. Phenomenological arguments yield microscopic potential relations of the form

$$W^{\mathrm{rep}}(\zeta) = \frac{B}{\|\zeta\|^{12}} \tag{45}$$

Please cite this article in press as: M. Lenczner, R.C. Smith, A two-scale model for an array of AFM's cantilever in the static case, Mathematical and Computer Modelling (2007), doi:10.1016/j.mcm.2006.12.028

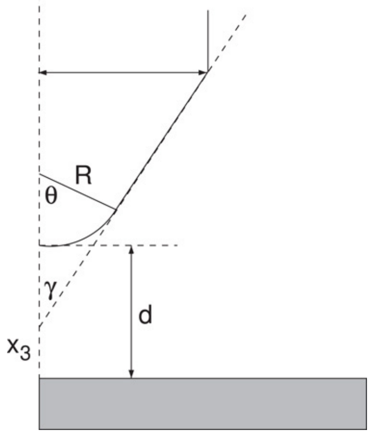

Fig. 4. Geometry of the AFM tip.

where B is a constant which depends on electronic and material properties of the sample and tip. Arguments analogous to those for the attractive forces yield short-range force relations analogous to (41) and (43), or (44).

6. Examples

An example illustrating the application of the thin plate model for an AFM is presented in Section 6.1. In Section 6.2, the two-scale model is applied to an AFM array. Finally, in Section 6.3, results for a simulation of the AFM array are reported and discussed.

6.1. A single AFM

The two-dimensional domain ω_P is a rectangle $\omega_P = (0, \ell_C^0) \times (0, L_C)$ with $\ell_C^0 << L_C$. The plate is made up of a homogeneous isotropic material, is clamped on the side $x_2 = 0$ and is left free otherwhere. The elastic part is $\omega_E = (0, \ell_C^0) \times (0, L_E)$ and the rigid part is its complementary set $\omega_R = (0, \ell_C^0) \times (L_E, L_C)$. The coordinates of the tip are $x^{\text{tip}} = (x_1^{\text{tip}}, x_2^{\text{tip}}, x_3^{\text{tip}})$. The shape of the sample to be analyzed is parameterized by a function $\phi(x_1, x_2)$. The force applied on the tip is modeled as a concentrated force

$$f(x) = F(d)\delta_{x^{\text{tip}}}(x)$$

where $d = u^{\text{tip}} - \phi^{\text{tip}}$ with $\phi^{\text{tip}} = \phi(x_1^{\text{tip}}, x_2^{\text{tip}})$ and $u^{\text{tip}} = u(x^{\text{tip}})$. We will assume that $F_1 = F_2 = 0$. If the dependency of u_3^P with respect to x_1 is neglected, then the distance d between the tip and the sample is solution of the nonlinear algebraic equation

$$(d + \phi^{\text{tip}}) - k^P(x_2^{\text{tip}})F_3(d) = 0 \tag{46}$$

and when d is known u_3^P is computed by

$$u_3^P(x_2) = k^P(x_2)F_3(d) \quad \text{for } x_2 \in [0, L_C]$$

where

$$\begin{aligned} k^P(x_2) &= \frac{x_2^2}{6m^P}(3x_2^{\text{tip}} - x_2) \quad \text{in } [0, L_E] \\ &= \frac{L_E}{6m^P}(2L_E^2 - 3x_2^{\text{tip}}L_E + (6x_2^{\text{tip}} - 3L_E)x_2) \quad \text{in } (L_E, L_C], \end{aligned}$$

and

$$m^P = \frac{8\mu a^3 \ell_C^0(\lambda + \mu)}{3(\lambda + 2\mu)}. \tag{47}$$

Please cite this article in press as: M. Lenczner, R.C. Smith, A two-scale model for an array of AFM's cantilever in the static case, Mathematical and Computer Modelling (2007), doi:10.1016/j.mcm.2006.12.028

The proof is straightforward and we mention only the main steps. From the definition of ξ^P, Ξ^P, f^P and g^P,

$$\xi^P = \int_{\Omega_R} f_3(x)\mathrm{d}x = F_3 \quad \text{and} \quad \Xi_2^P = \int_{\Omega_R} f_3(x)x_2 - f_2(x)x_3\mathrm{d}x = F_3 x_2^{\text{tip}} - F_2 x_3^{\text{tip}} = F_3 x_2^{\text{tip}}$$

because $F_2 = 0$. The displacement u_3^P is solution of the boundary value problem

$$\begin{aligned} &\frac{\mathrm{d}^4 u_3^P}{\mathrm{d}x_2^4}(x_2) = 0 \quad \text{for } x_2 \in (0, L_E), \qquad u_3^P(0) = \frac{\mathrm{d}u_3^P}{\mathrm{d}x_2}(0) = 0 \\ &-m^P \frac{\mathrm{d}^3 u_3^P}{\mathrm{d}x_2^3}(L_E) = \xi^P \quad \text{and} \quad m^P \left(\frac{\mathrm{d}^2 u_3^P}{\mathrm{d}x_2^2} - \frac{\mathrm{d}^3 u_3^P}{\mathrm{d}x_2^3} x_2 \right)(L_E) = \Xi_2^P \end{aligned} \tag{48}$$

where $m^P = \ell_C^0 R_{2222}^P$. In the rigid part

$$u_3^P(x_2) = b^P + B_2^P x_2$$

with

$$b^P = u_3^P(L_E) - \frac{\mathrm{d}u_3^P}{\mathrm{d}x_2}(L_E)L_E \quad \text{and} \quad B_2^P = \frac{\mathrm{d}u_3^P}{\mathrm{d}x_2}(L_E).$$

In particular,

$$u^{\text{tip}} = b^P + B_2^P x_2^{\text{tip}}.$$

Eq. (48) yields $u_3^P(x_2) = a_0 + a_1 x_2 + a_2 x_2^2 + a_3 x_2^3$ in the elastic part with

$$a_0 = a_1 = 0, \quad 2m^P a_2 = \Xi_2^P \quad \text{and} \quad -6m^P a_3 = \xi^P \tag{49}$$

from which the equation $u_3^P(x_2) = k^P(x_2)F_3(d)$ follows. The equation for d follows by taking $x_2 = x_2^{\text{tip}}$ and using the relation $u_3^P(x_2^{\text{tip}}) = d + \phi^{\text{tip}}$.

6.2. An AFM array

The whole system is still comprised of a homogeneous isotropic material. The subdomains Y_B and Y_C are two rectangles described respectively in the coordinates (O_B, y_1^B, y_2^B) and (O_C, y_1^C, y_2^C) by

$$Y_B = (0, 1) \times (0, \ell_B) \quad \text{and} \quad Y_C = (0, \ell_C^0) \times (0, L_C)$$

where $O_C = (-\frac{\ell_C^0}{2}, \ell_B - \frac{1}{2})$, $O_B = (-\frac{1}{2}, -\frac{1}{2})$, $y^B = y - O_B$ and $y^C = y - O_C$; see Fig. 5 for the description of the cell and Fig. 6 for the changes of coordinates. The flexible part Y_F of Y_C is $(0, \ell_C^0) \times (0, L_F)$ in (O_C, y^C).

We assume that $\gamma_1^M = \varnothing$ so $\gamma_0^M = \{0, 1\} \times (0, 1)$. The tip coordinates are denoted by y^{tip} in (O, y_1, y_2), by y^{Ctip} in (O, y_1^C, y_2^C) and by $x_i^{\text{tip}} = (x_{i1}^{\text{tip}}, x_{i2}^{\text{tip}}, x_{i3}^{\text{tip}})$ in Ω_P.

The force applied to the cantilever is assumed to be concentrated on each tip, so that

$$f_3(x) = \sum_i F_3^i \delta_{x_i^{\text{tip}}}(x)$$

with $F_3^i = F_3(u_3(x_i^{\text{tip}}) - \phi(x_{1i}^{\text{tip}}, x_{2i}^{\text{tip}}))$. We still assume that $f_1 = f_2 = 0$. Then for $d(x) = u^M(x) + u^C(x, y^{\text{Ctip}}) - \phi(x)$, the two-scale model is stated as follows. The couple (d, u^M) is a solution of

$$R^{\text{beam}} \partial^4_{x_1 x_1 x_1 x_1} u^M(x) = f^{\text{beam}}(x) \quad \text{for all } x \in \omega \tag{50}$$

$$u^M(0, x_2) = u^M(L_1, x_2) = \partial_{x_1} u^M(0, x_2) = \partial_{x_1} u^M(L_1, x_2) = 0 \quad \text{for all } x_2 \in (0, L_2)$$

and

$$(d + \phi - u^M)(x) - k^C(y_2^{\text{Ctip}}) f^{\text{beam}}(x) = 0 \quad \text{for all } x \in \omega. \tag{51}$$

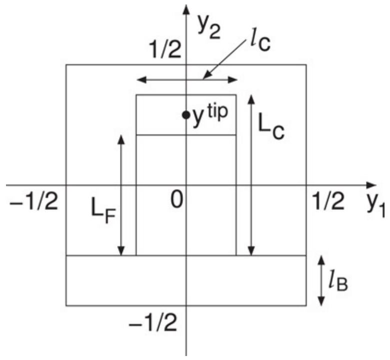

Fig. 5. Reference cell.

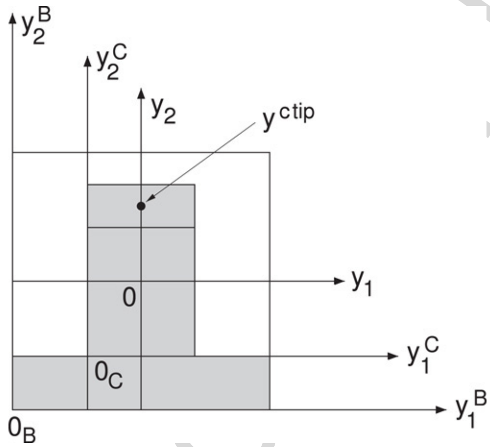

Fig. 6. Local coordinates in Y_B and Y_C.

Once d is known, u^C is computed by

$$u^C(x, y_2) = k^C(y_2^C) f^{\text{beam}}(x) \quad \text{for all } (x, y_2^C) \in \omega \times (0, L_C)$$

$$\begin{aligned} k^C(y_2^C) &= \frac{y_2^{C2}}{6m^C}(3y_2^{\text{Ctip}} - y_2^C) \quad \text{in } [0, L_F] \\ &= \frac{L_F}{6m^C}(2L_F^2 - 3y_2^{\text{Ctip}} L_F + (6y_2^{\text{Ctip}} - 3L_F)y_2^C) \quad \text{in } (L_F, L_C], \end{aligned}$$

where the rigidity per unit length is

$$R^{\text{beam}} = \varepsilon R_{11}^M = \frac{4\varepsilon\mu a_B^3 \ell_B}{3(\lambda + 2\mu)} \left(2\lambda + 2\mu - \frac{\lambda^2}{2(\lambda + \mu)}\right)$$

and

$$m^C = \frac{8\varepsilon^{-2} a_C^3 \ell_C^0 \mu(\lambda + \mu)}{3(\lambda + 2\mu)}.$$

The force per unit length $f^{\text{beam}} = \varepsilon^{-1} F_3^i$ in the ith cell. When d and F_3 are continuous one may use the continuous force distribution

$$f^{\text{beam}}(x) \approx \frac{1}{\varepsilon} F_3(d(x)).$$

Moreover, $\mathcal{L}^B(\nabla\nabla^{\mathrm{T}} u^M) = -\frac{2\lambda}{4(\lambda+\mu)} \begin{pmatrix} 0 & 0 \\ 0 & 1 \end{pmatrix}$ and $\theta = 0$.

Please cite this article in press as: M. Lenczner, R.C. Smith, A two-scale model for an array of AFM's cantilever in the static case, Mathematical and Computer Modelling (2007), doi:10.1016/j.mcm.2006.12.028

Let us sketch the derivation. The first step consists in choosing f^0. It is necessarily concentrated in $y = y^{\text{tip}}$, so

$$f^0(x, y) \approx \varepsilon^{-2} F_3(d(x))\delta_{y^{\text{tip}}}(y) \quad \text{in the } i\text{th cell,}$$

the choice of its coefficients being justified by the fact that $\int_{Y_R} f^0(x, y)\mathrm{d}y = F_3^i + O(\varepsilon)$. Indeed, $f^0 = \widehat{f}^P + O(\varepsilon)$, $f^P = \int_{-h}^{a} f_3 \mathrm{d}x_3$ and $f_3 = \sum_i F_3^i \delta_{x_i^{\text{tip}}}$; then

$$\begin{aligned}\int_{Y_P} f^0 \mathrm{d}y &= \varepsilon^{-2} \int_{Y_i^\varepsilon \cap \omega_P} f^P + O(\varepsilon)\mathrm{d}x \\ &= \varepsilon^{-2} \int_{Y_i^\varepsilon \cap \omega_P} \int_{-h}^{a} f_3 + O(\varepsilon)\mathrm{d}x_3\mathrm{d}x = \varepsilon^{-2} F_3^i + O(\varepsilon) \quad \text{in the } i\text{th cell}\end{aligned}$$

which may be approximated by $\varepsilon^{-2} F_3(d(x))$.

With that choice of f^0, one may derive the solutions of the three Problems $\mathcal{P}^B$, $\mathcal{P}^M$ and $\mathcal{P}^C$.

Problem $\mathcal{P}^B$. The solution w^B of $\mathcal{P}^B$ is

$$w^B(y^B) = -\frac{\lambda\nu}{4(\lambda+\mu)}(y_1^B)^2.$$

This is verified by showing that such w^B satisfies the variational formulation. Thus

$$M^B = \frac{8\mu K}{3(\lambda+2\mu)}\begin{pmatrix}\lambda & 0\\ 0 & 2(\lambda+2\mu)\end{pmatrix} \quad \text{with } K = -\frac{\lambda\nu}{4(\lambda+\mu)}$$

and

$$\int_{Y_B} M^B \nabla_y \nabla_y^{\mathrm{T}} v \mathrm{d}y = \frac{16\mu(\lambda+\mu)K}{3(\lambda+2\mu)} \int_{Y_B} \partial^2_{y_1 y_1} v \mathrm{d}y$$

because $\int_{Y_B} \partial^2_{y_2 y_2} v\mathrm{d}y = 0$ due to the periodicity of $\partial_{y_1} v$ on γ_{per}. By another way,

$$F^B = \frac{4\mu}{3}\left(\frac{\nu}{\lambda+2\mu}\begin{pmatrix}2(\lambda+\mu) & 0\\ 0 & \lambda\end{pmatrix} + \begin{pmatrix}0 & \alpha\\ \alpha & 0\end{pmatrix}\right);$$

then

$$\int_{Y_B} F^B \nabla_y \nabla_y^{\mathrm{T}} v \mathrm{d}y = \frac{4\mu\lambda\nu}{3(\lambda+2\mu)} \int_{Y_B} \partial^2_{y_2 y_2} v \mathrm{d}y$$

because $\int_{Y_B} \partial^2_{y_1 y_1} v\mathrm{d}y = \int_{Y_B} \partial^2_{y_1 y_2} v\mathrm{d}y = 0$ due to the periodicity of v and $\partial_{y_1} v$. Finally the variational formulation

$$\int_{Y_B} M^B \nabla_y \nabla_y^{\mathrm{T}} v \mathrm{d}y = -\int_{Y_B} F^B \nabla_y \nabla_y^{\mathrm{T}} v \mathrm{d}y$$

is fulfilled.

Problem $\mathcal{P}^M$. It is straightforward to verify that

$$\begin{aligned}\mathcal{L}^B_{\xi\zeta\gamma\delta} &= -\frac{2\lambda}{4(\lambda+\mu)}\delta_{\xi 2}\delta_{\zeta 2}\delta_{\gamma 1}\delta_{\rho 1}\\ \widetilde{R}^M_{\alpha\beta\gamma\rho} &= \frac{4\mu\ell_B a_B^3}{3}\left(\frac{\lambda}{\lambda+2\mu}\delta_{\alpha\beta}\delta_{\gamma\rho} + \delta_{\alpha\gamma}\delta_{\beta\rho} - \frac{\lambda}{2(\lambda+\mu)}\left(\frac{\lambda}{\lambda+2\mu}\delta_{\alpha\beta}\delta_{\gamma 1}\delta_{1\rho} + \delta_{\alpha 2}\delta_{2\beta}\delta_{\gamma 1}\delta_{1\rho}\right)\right).\end{aligned}$$

It then follows that

$$R^M = \begin{pmatrix}\widetilde{R}^M_{1111} & 0\\ 0 & \dfrac{16\ell_B\mu}{3}\end{pmatrix} \quad \text{with } \widetilde{R}^M_{1111} = \frac{4\ell_B\mu a_B^3}{3(\lambda+2\mu)}\left(2\lambda + 2\mu - \frac{\lambda^2}{2(\lambda+\mu)}\right).$$

Please cite this article in press as: M. Lenczner, R.C. Smith, A two-scale model for an array of AFM's cantilever in the static case, Mathematical and Computer Modelling (2007), doi:10.1016/j.mcm.2006.12.028

The macroscopic forces are $f_1^M(x) = F_3(d(x))$ and $f_2^M = 0$, so u^M is a solution of the boundary value problem (50) and θ is a solution of

$$\partial^2_{x_1x_1}\theta(x) = 0 \quad \text{for } x \in \omega, \qquad \theta(0, x_2) = \theta(1, x_2) = 0 \quad \text{for all } x_1 \in (0, 1);$$

thus $\theta = 0$.

Problem $\mathcal{P}^C$. The calculations are similar to those for the simple plate model in Section 6.1. Neglecting the variations of u^C with respect to y_1 it turns out that u^C depends only on x and y_2 and is a solution of the boundary value problem

$$\frac{\partial^4 u^C}{\partial y_2^4} = 0 \quad \text{for } y_2^C \in (0, L_F), \qquad u^C = \frac{\partial u^C}{\partial y_2} = 0 \quad \text{for } y_2^C = 0 \tag{52}$$

$$-\ell_C R^C_{2222}\frac{\partial^3 u^C}{\partial y_2^3} = \xi^C \quad \text{and} \quad \ell_C R^C_{2222}\left(\frac{\partial^2 u^C}{\partial y_2^2} - \frac{\partial^3 u^C}{\partial y_2^3} y_2^C\right) = \Xi_2^C \quad \text{for } y_2^C = L_F$$

and

$$\xi^C(x) = \varepsilon^{-2}F_3(d(x)), \qquad \Xi_2^C(x) = \varepsilon^{-2}F_3(d(x))y_2^{\text{tip}}.$$

The expression of u^C follows by using the fact that $R^C = \varepsilon^{-4}R^P$. Finally, by using the relation $u^C(., y_2) = d - u^M + \phi$ for $y_2^C = y_2^{\text{Ctip}}$, Eq. (51) follows.

6.3. Numerical simulation of the AFM array

For numerical computation the algebraic equation (51) is replaced by

$$(d + \phi - u^M)(R + d - R\sin(\gamma))^2 d^2 - k^C(y_2^{\text{Ctip}})G(d) = 0 \tag{53}$$

where $G(d) = F_3(d)(R + d - R\sin(\gamma))^2 d^2$. $F_3(d) = F^{vdW}(d) + F^{\text{rep}}(d)$ where the van der Waals force F^{vdW} is defined in (44) from the potential (36) and the repulsive force F^{rep} is built from (45) in the same way. In order to avoid numerical errors due to the presence of large and small values in the system, we use the normalized functions and variables

$$x_1^* = x/L_1, \qquad x_2^* = x_2/L_2, \qquad u^{M*}(x^*) = u^M(x)/\phi_{\text{scal}}, \qquad d^*(x^*) = d(x)/\phi_{\text{scal}},$$
$$\phi^*(x^*) = \phi(x)/\phi_{\text{scal}}, \qquad F^*(d^*) = L_1^4 F_3(d^*\phi_{\text{scal}})/(R^{\text{beam}}\phi_{\text{scal}}\varepsilon),$$
$$G^*(d^*) = G(d^*\phi_{\text{scal}})/\phi^3_{\text{scal}}, \qquad R^* = R/\phi_{\text{scal}}, k^* = k^C(y_2^{\text{Ctip}})/\phi^2_{\text{scal}}$$

so that (50) and (53) are replaced by

$$\partial^4_{x_1^*}u^{M*} = F^*(d^*) \quad \text{and} \quad E(d^*, u^{M*}) = 0 \quad \text{in}(0, 1)^2$$
$$u^{M*}(x^*) = \partial_{x_1}u^{M*}(x^*) = 0 \quad \text{for all } x^* \in \{0, 1\} \times (0, 1)$$

with $E(d^*, u^{M*}) = (d^* + \phi^* - u^{M*})(R^* + d^* - R^*\sin(\gamma))^2(d^*)^2 - k^*G^*(d^*)$. The displacement u^{M*} is decomposed on the basis of eigenfunctions $\psi_m(x_1^*)$:

$$u^{M*}(x^*) = \sum_{n=1}^{N_u} U_n(x_2^*)\psi_n(x_1^*)$$

where

$$\partial^4_{x_1^*}\psi_n(x_1^*) = \lambda_n\psi_n(x_1^*) \quad \text{for all } x_1^* \in (0, 1) \text{ and } \psi_n(x_1^*) = \partial_{x_1}\psi_n(x_1^*) = 0 \text{ for } x_1^* \in \{0, 1\};$$

then

$$U_n(x_1^*) = \int_0^1 F^*(d^*(x^*))\psi_n(x_1^*)\mathrm{d}x_1^*/\lambda_n. \tag{54}$$

Please cite this article in press as: M. Lenczner, R.C. Smith, A two-scale model for an array of AFM's cantilever in the static case, Mathematical and Computer Modelling (2007), doi:10.1016/j.mcm.2006.12.028

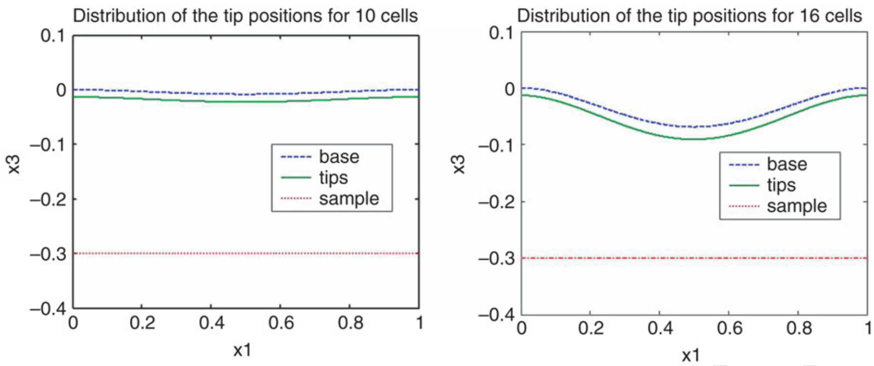

Fig. 7. Distributions of u^{M*}, $u^{M*}+\overline{u}^{C*}$ and of ϕ^* as functions of x_1^* for 10, 16 cantilevers.

The functions ϕ^* and d^* are decomposed on the normalized orthogonal Chebychev polynomials P_n on (0, 1):

$$\phi^*(x_1^*)=\sum_{n=1}^{N_\phi}\Phi_n(x_2^*)P_{n-1}(x_1^*)\quad\text{and}\quad d^*(x_1^*)=\sum_{n=1}^{N_d}D_n(x_2^*)P_{n-1}(x_1^*).$$

Thus the second equation is replaced by

$$\mathcal{E}(\mathcal{D},\,\Phi,\mathcal{U})=\prime$$

where

$$\mathcal{E}(\mathcal{D},\,\Phi,\mathcal{U})=\mathcal{E}\left(\sum_{\backslash=\infty}^{\mathcal{N}_\lceil}\mathcal{D}_\backslash(\S_\in^*)\mathcal{P}_{\backslash-\infty}(\S_\infty^*),\ \sum_{\backslash=\infty}^{\mathcal{N}_\phi}\Phi_\backslash(\S_\in^*)\mathcal{P}_{\backslash-\infty}(\S_\infty^*),\ \sum_{\backslash=\infty}^{\mathcal{N}_\sqcap}\mathcal{U}_\backslash(\S_\in^*)\psi_\backslash(\S_\infty^*)\right).$$

The discretized system is solved by replacing U_n by its expression (54) and then by searching the minimum of $\int_0^1\mathcal{E}^2(D,\,\Phi,\,U)\mathrm{d}x_1^*$ with respect to D. The minimum search is conducted by combining a minimizing method relative to D and a length line continuation with respect to the number of cells. The algorithm is initialized with a small number of cells where u^{M*} is close to zero. Then the number of cells is increased incrementally.

We have conducted computations with a square cell having a length of $\varepsilon = 50$ μm. The other parameters are $L_C = 0.5$, $\ell_C^0 = 1/16$, $a_C = \varepsilon 40$ μm, $y_2^{\mathrm{Ctip}} = 7/16$, $L_F = 3/8$, $\ell_B = 1/4$, $a_B = \varepsilon/10$ μm, $A = 1.25\mathrm{e}{-19}$ J, $\gamma = \pi/6$, $R = 10^{-7}$ m, $\lambda = 6.1\mathrm{e}11$, $\mu = 5.2\mathrm{e}11$, $\phi_{\mathrm{scal}} = 10^{-9}$. The number of cantilevers or equivalently the length of the array is a parameter chosen in each experiment. In the following we refer to three choices of ϕ^* corresponding to three values of N_ϕ:

$$N_\phi = 1 : \phi^*(x_1^*) = \frac{\phi^{0*}+\phi^{1*}}{2},$$

$$N_\phi = 2 : \phi^*(x_1^*) = \phi^{0*} + (\phi^{1*}-\phi^{0*})x_1^*,$$

$$N_\phi = 3 : \phi^*(x_1^*) = \phi^{0*} + 4\phi^{1*}x_1^*(1-x_1^*)$$

where $\phi^{0*} = -0.3$ and $\phi^{1*} = -0.4$.

Fig. 7 represents the functions u^{M*}, $u^{M*}+\overline{u}^{C*}$ at the tip locations and of ϕ^* of $x_1^* \in (0, 1)$ in the case of a flat sample, $N_\phi = 1$, for two arrays having 10 and 16 cantilevers in the direction x_1. It is not surprising to observe that when the base length increases it deforms in a non-negligible way in comparison with the total displacement of the tip.

Fig. 8 illustrates how the maximum value over x_1^* of the ratio $\frac{u^{M*}}{u^{M*}+\overline{u}^{C*}}$ taken at the tips varies as a function of the number of cells for $N_\phi = 1$. Evidently this ratio tends to zero for a small number of cells but it also increases dramatically with the number of cells, which means that in this case the tip displacement is more governed by the base displacement than by the cantilever deflection.

Please cite this article in press as: M. Lenczner, R.C. Smith, A two-scale model for an array of AFM's cantilever in the static case, Mathematical and Computer Modelling (2007), doi:10.1016/j.mcm.2006.12.028

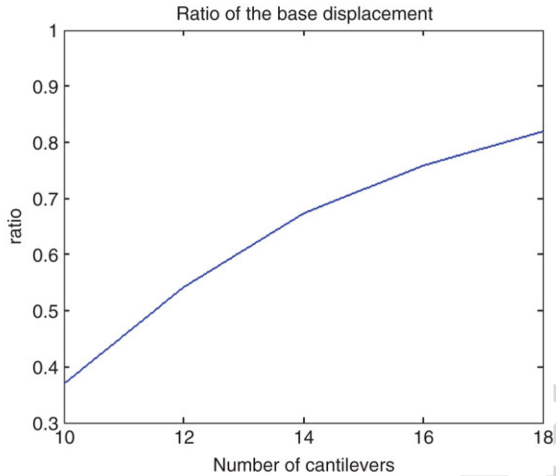

Fig. 8. $\max_{x^*} \frac{u^{M*}}{u^{M*}+\overline{u}^{C*}}$ with respect to the number of cells.

Table 1
Err for 10 cells and 14 cells depending on N_ϕ and N_d

$N_\phi \setminus N_d$	1	3	5	7	9	$N_\phi \setminus N_d$	1	3	5	7	9
1	2.2	2.8	4.3	5.7	7.4	1	1.5	2.1	3.6	4.9	5.8
2	1.0	2.8	3.7	3.8	3.9	2	1.0	2.1	3.6	4.6	4.7
3	0.7	2.7	3.4	4.0	4.7	3	0.6	2.5	3.4	4.0	4.1

The quality of the approximation of d^* by using the Chebychev polynomials is also of interest. In Table 1, we report the order of magnitude of the error on d^*

$$\text{Err} = -\log_{10} \text{err} \quad \text{where } \text{err}^2 = \frac{\int_0^1 (d^*_{N_d}(x_1^*) - d^*(x_1^*))^2 \mathrm{d}x_1^*}{\int_0^1 (d^*(x_1^*))^2 \mathrm{d}x_1^*}$$

as a function of the number N_d of polynomials used.

7. Conclusion

We have derived two-scale models of AFM arrays which take into account the deformations of the base coupled with those of the cantilevers. The first model is a general one and can be discretized with a Finite Element Method for both the macroscopic domain and the reference cell. The second model is a particular case where hand calculations have been pushed at their limit, so it has the form of a Euler–Bernoulli beam equation, associated to the base, coupled with a nonlinear algebraic equation for the cantilevers. They do not require a heavy Finite Elements implementation and may provide an efficient model for a designer. The derivation of the general model is based on an asymptotic approach which guarantees a good confidence in its results. Let us review the features of the general model. The cantilevers are modeled with a Love–Kirchhoff thin plate model which allows one to describe general plate flexions encountered for example in nanomanipulation, their tip is rigid, the atomic forces are really applied to the extremity of the tip and the base is assumed to be much stiffer than the cantilevers, which simplifies the model significantly. The results show that, even for a small number of cantilevers, the mechanical displacement of the base cannot be neglected in a design process. Our perspectives consist in completing this work in several aspects including the dynamics, realistic shapes of the sample and control of the whole system.

Uncited references

Fig. 4. [25].

Acknowledgement

The research of R.C. Smith was supported in part by the Air Force Office of Scientific Research through the grant AFOSR-FA9550-04-1-0203.

Appendix A

In this appendix, we report some mathematical definitions and properties. The concepts of weak and strong approximation are defined in Appendix A.1. Then in Appendix A.2 the two-scale transform of a function is defined and its elementary properties are stated. Then, in Appendix A.3 some approximation of the adjoint of the two-scale transform are derived. Some weak approximations of the two-scale transform of the first-order and the second-order derivatives are derived in Appendix A.4. Finally, a fundamental inequality used for the derivation of the two-scale model is stated and proved in Appendix A.5.

A.1. Weak and strong approximation

Consider an open measurable set $A \subset \mathbb{R}^n$, $w^\varepsilon \in L^2(A)$, a function depending on the parameter ε and a function $w^0 \in L^2(A)$ independent of ε. We say that $w^\varepsilon = w^0 + O(\varepsilon)$ weakly in $L^2(A)$ if $\int_A (w^\varepsilon - v^0) v \mathrm{d}x = O(\varepsilon)$ for all $v \in L^2(A)$ and we say that the same equality holds strongly in $L^2(A)$ if $\int_A (w^\varepsilon - w^0)^2 \mathrm{d}x = O(\varepsilon)$.

For example the oscillating function $\sin(\frac{x}{\varepsilon})$ can be approximated by zero in the weak sense but cannot be approximated by a function independent of ε in the strong sense.

A.2. Properties of the two-scale transform

We state here some elementary properties of the two-scale transform. The proofs are elementary and are not detailed here. Some may be found in Lenczner and Senouci-Bereski [11]. They are stated in the general case where $Y = (-\frac{1}{2}, \frac{1}{2})^d$ and $\omega = \Pi_{j=1}^d (0, L_j)$ with d any positive integer and L_i some non-negative numbers so that ω contains an entire number of cells Y_i of size ε^d. The cells Y_i are indexed by the multi-indices $i = (i_1, \ldots, i_d)$.

Two-scale transform of functions defined in ω: The definition of the two-scale transforms of a function v defined in ω remains formally the same as in (15):

$$\widehat{v}(x, y) = \sum_i \chi_{Y_i^\varepsilon}(x) v(x_i^\varepsilon + \varepsilon y)$$

and has the simple properties,

$$\widehat{v + w} = \widehat{v} + \widehat{w}, \qquad \widehat{vw} = \widehat{v}\widehat{w}, \qquad \widehat{\nabla v} = \frac{1}{\varepsilon}\nabla_y \widehat{v} \quad \text{and} \quad \int_\omega v(x)\mathrm{d}x = \int_{\omega\times Y} \widehat{v}(x, y)\mathrm{d}y\mathrm{d}x.$$

It follows that $v, w \in L^2(\omega)$

$$\|v\|_\omega = \|\widehat{v}\|_{\omega\times Y} \quad \text{and} \quad \int_\omega vw\mathrm{d}x = \int_{\omega\times Y} \widehat{v}\widehat{w}\mathrm{d}y\mathrm{d}x. \tag{55}$$

The two-scale transform defined from $L^2(\omega)$ to $L^2(\omega \times Y)$ is a linear operator that we denote by T. Its adjoint T^* is defined by

$$\int_\omega (T^* v)(x) w(x)\mathrm{d}x = \int_{\omega\times Y} v(x, y)(Tw)(x, y)\mathrm{d}x\mathrm{d}y \tag{56}$$

for all $w \in L^2(\omega)$ and $v \in L^2(\omega \times Y)$. A direct computation shows that T^* is defined through

$$T^* v(x_i + \varepsilon y) = \int_{Y_i^\varepsilon} v(z, y)\mathrm{d}z \quad \text{for all } y \in Y \text{ and all cell centers } x_i$$

or through its global expression

$$T^*v(x) = \sum_i \varepsilon^{-d} \int_{Y_i^\varepsilon} v\left(z, \frac{x - x_i}{\varepsilon}\right) \mathrm{d}z \chi_{Y_i^\varepsilon}(x). \tag{57}$$

Moreover,

$$T^*\widehat{v} = v. \tag{58}$$

Indeed, for all $w \in L^2(\omega)$, $\int_\omega (T^*\widehat{v} - v) w \mathrm{d}x = \int_{\omega\times Y} \widehat{v}\widehat{w} \mathrm{d}y\mathrm{d}x - \int_\omega vw\mathrm{d}x = 0$ from (55). When $\widehat{v}$ may be approximated through

$$\widehat{v} = v^0 + O(\varepsilon), \tag{59}$$

the inversion formula provides an approximation of v:

$$v = T^*v^0 + O(\varepsilon). \tag{60}$$

Two-scale transform of functions defined in $\omega_1 \subset \omega$: Consider a εY-periodic set $\omega_1 \subset \omega$ with cells Y_{1i}^ε and the associated unit cell $Y_1 \subset Y$. From the basic equality

$$\widehat{\chi_{\omega_1}} = \chi_{\omega\times Y_1},$$

it follows that

$$\int_{\omega_1} v(x)\mathrm{d}x = \int_{\omega\times Y_1} \widehat{v}(x, y)\mathrm{d}y\mathrm{d}x$$

where $\widehat{v}$ represents the two-scale transform of the function v extended by zero to ω. Then for $v \in L^2(\omega)$

$$\|v\|_{\omega_1} = \|\widehat{v}\|_{\omega\times Y_1}.$$

For $u \in L^2(\omega_1)$ and $v \in L^2(\omega \times Y_1)$,

$$\int_{\omega_1} uT^*v\mathrm{d}x = \int_{\omega\times Y_1} \widehat{u}v\mathrm{d}y\mathrm{d}x \tag{61}$$

where v has been extended by zero to $\omega \times Y$ prior to applying T^*. Finally, the approximation (60) still holds.

Two-scale transform on the boundary: The boundary of ω is denoted by γ and γ_1 represents the intersection between the closure of ω_1 and γ. In the same way, γ_{per} represents the boundary of Y and γ_{per} the intersection between γ^Y and the closure of Y_1. The outward unit normal vectors to the boundaries of ω and Y are denoted by n_x and n_y. Then

$$\int_{\gamma_1} v\mathrm{d}s(x) = \int_{\gamma*\gamma_{\text{per}}} \widehat{v}\mathrm{d}s(x)\mathrm{d}s(y)$$

where

$$\gamma * \gamma_{\text{per}} = \{(x, y) \in \gamma \times \gamma_{\text{per}} / n_x(x) = n_y(y)\}$$

and where the definition of $\widehat{v}$ has been extended continuously to the boundary. Moreover, if v is continuously differentiable then

$$\int_{\gamma_1} uT^*v\mathrm{d}s(x) = \int_{\gamma*\gamma_{\text{per}}} \widehat{u}v\mathrm{d}s(y)\mathrm{d}s(x) + O(\varepsilon). \tag{62}$$

Extension to some generalized functions: The two-scale transform is a linear operator that is well defined on functions. Its definition can also be extended to some generalized functions or distributions: v being such a generalized function, Tv is defined formally by the duality

$$\int_\omega \langle Tv, w\rangle_y \,\mathrm{d}x = \langle v, T^*w\rangle_x$$

for all w belonging to a class of regular functions defined on $\omega \times Y$. From this definition the two-scale transform of

$$v(x) = g(x) \sum_i \delta_{x_i + \varepsilon y^0}(x)$$

Tv is found to be

$$Tv(x, y) = \varepsilon^{-d} Tg(x, y) \delta_{y^0}(y) \tag{63}$$

where $y^0 \in Y$, δ_ξ is the Dirac distribution in ξ and g is any regular function. Indeed,

$$\begin{aligned}
\langle v, T^* w\rangle_x &= \left\langle g(x) \sum_i \delta_{x_i+\varepsilon y^0}(x), \sum_j \varepsilon^{-d} \int_{Y_j^\varepsilon} \overline{w}\left(z, \frac{x}{\varepsilon}\right) \mathrm{d}z \chi_{Y_j^\varepsilon}(x) \right\rangle_x \\
&= \sum_i g(x_i + \varepsilon y^0) \varepsilon^{-d} \int_{Y_i^\varepsilon} w(z, y^0) \mathrm{d}z = \varepsilon^{-d} \sum_i \int_{Y_i^\varepsilon} Tg(z, y^0) w(z, y^0) \mathrm{d}z \\
&= \varepsilon^{-d} \int_\omega Tg(z, y^0) w(z, y^0) \mathrm{d}z = \varepsilon^{-d} \int_\omega \left\langle Tg(z, y) \delta_{y^0}(y), w(z, y^0) \right\rangle_y \mathrm{d}z.
\end{aligned}$$

This means that $Tv(z, y) = \varepsilon^{-d} Tg(z, y) \delta_{y^0}(y)$.

A.3. Approximation of T^*

From its definition (57), T^* is not a regular function. For various reasons, we need a regular approximation of T^*v that will be denoted by $\overline{v}$. The expression of $\overline{v}$ depends on the regularity of v with respect to its first variable. Prior to defining $\overline{v}$, it is required to extend $v(x, y)$ to $y \in \mathbb{R}^d$ by Y-periodicity by posing $v(x, y + z) = v(x, y)$ for any $z \in \mathbb{Z}^d$ and $y \in Y$.

Case where v is regular: If v is $k + 1$ times continuously differentiable with respect to its first variable then T^*v can be approximated up to the order k with an expansion in ε,

$$T^* v = \sum_{j=0}^k f_j \varepsilon^j + \varepsilon^k O(\varepsilon) \tag{64}$$

whose first coefficients are

$$f_0 = \overline{v}, \qquad f_1 = -X.\overline{\nabla_x v} \quad \text{and} \quad f_2 = \frac{1}{2} X^{\mathrm{T}} (\overline{\nabla_x \nabla_x^{\mathrm{T}} v}) X + \frac{1}{12} \overline{\Delta_x v} \quad \text{with } X = T^*(y) \tag{65}$$

and

$$\overline{v}(x) = v\left(x, \frac{x}{\varepsilon} - \frac{1}{2}\right). \tag{66}$$

The calculation of these coefficients is straightforward. Indeed, one starts by applying the Taylor formula to v at (x, y) with respect to its first variable: $v(z, y) = v(x, y) + \nabla_x v(x, y)(z - x) + \frac{1}{2}(z - x)^{\mathrm{T}} \nabla_x \nabla_x^{\mathrm{T}} v(x, y)(z - x) + \varepsilon^2 O(\varepsilon)$ for $x, z \in Y_i^\varepsilon$. Then one substitutes it in the expression of T^*v. The calculations of the integrals are carried out by using the decomposition $z - x = (z - x_i^\varepsilon) + (x_i^\varepsilon - x)$ and the identities $\int_{Y_i^\varepsilon} (z - x_i^\varepsilon) \mathrm{d}z = 0$ and $\sum_i \chi_{Y_i^\varepsilon}(x) = 1$.

Conversely one deduces an approximation of $\overline{v}$:

$$\overline{v} = T^* \left(v + \varepsilon (y.\nabla_x) v + \frac{\varepsilon^2}{2} (y.\nabla_x)^2 v - \frac{\varepsilon^2}{24} \Delta_x v \right) + \varepsilon^2 O(\varepsilon), \tag{67}$$

which is derived by applying the second-order approximation (64) and replacing $\overline{\nabla_x \nabla_x^{\mathrm{T}} v}$, $\overline{\Delta_x v}$ with their zero-order approximations and $\overline{\nabla_x \nabla_y^{\mathrm{T}} v}$ with its first-order approximation.

The expressions of the derivatives of $\overline{v}$ with respect to those of v are of interest for a number of calculation and are easy to compute:

$$\nabla\overline{v} = \overline{\nabla_x v} + \frac{1}{\varepsilon}\overline{\nabla_y v}. \tag{68}$$

From (61) and (62) and the zero-order approximation of $T^* v$ by $\overline{v}$ one gets directly the approximations

$$\int_{\omega_1} u\overline{v}\mathrm{d}x = \int_{\omega\times Y_1}\widehat{u}v\mathrm{d}x\mathrm{d}y + O(\varepsilon) \quad \text{and} \quad \int_{\gamma_1} u\overline{v}\mathrm{d}s(x) = \int_{\gamma*\gamma_{\mathrm{per}}}\widehat{u}v\mathrm{d}s(y)\mathrm{d}s(x) + O(\varepsilon). \tag{69}$$

The approximation (60) has the drawback of suffering from a lack of regularity. In practice, it is preferable to replace it by $\overline{v}$:

$$v = \overline{v}^0 + O(\varepsilon) \tag{70}$$

provided that (59) holds true.

Case where v is partially regular: For some reasons explained in the forthcoming subsection Appendix A.4, we have to deal with cases where v is regular in some directions only. So we split any vector $x \in \mathbb{R}^d$ into two parts, $x = x^C + x^{NC}$, related respectively to the directions of differentiability indexed by C and the others indexed by NC. The choice of notations C and NC is motivated in Appendix A.4. So we use the decompositions $\nabla = \nabla^C + \nabla^{NC}$, $y = y^C + y^{NC}$ and $n = n^C + n^{NC}$. The dimensions of the linear spaces generated by x^C and x^{NC} are respectively d^C and d^{NC} so that $d^C + d^{NC} = d$. According to these notations, a cell Y_i^ε is split into the product $Y_i^{\varepsilon C} \times Y_i^{\varepsilon NC}$. Let us introduce

$$\overline{v}(x) = \varepsilon^{-d^{NC}} \int_{Y_i^{\varepsilon NC}} v\left(x^C + z^{NC}, \frac{x}{\varepsilon} - \frac{1}{2}\right)\mathrm{d}z^{NC}. \tag{71}$$

If v is $k+1$ times differentiable in the directions x^C then the approximation (64) still holds with

$$f_0 = \overline{v}, \qquad f_1 = -X.\overline{\nabla_x^C v} \quad \text{and} \quad f_2 = \frac{1}{2}X^{\mathrm{T}}(\overline{\nabla_x^C \nabla_x^{CT} v})X + \frac{1}{12}\overline{\Delta_x^C v} \quad \text{with } X = T^*(y^C) \tag{72}$$

instead of (65) but with $\overline{v}$ defined by (71) instead of (66), Δ_x^C meaning the Laplacian with respect to the direction x^C only. Conversely $\overline{v}$ is approximated by

$$\overline{v} = T^*\left(v + \varepsilon(y^C.\nabla_x^C)v + \frac{\varepsilon^2}{2}(y^C.\nabla_x^C)^2 v - \frac{\varepsilon^2}{24}\Delta_x^C v\right) + \varepsilon^2 O(\varepsilon).$$

The expression (68) of the derivatives of $\overline{v}$ is replaced by

$$\nabla^C\overline{v} = \overline{\nabla_x^C v} + \frac{1}{\varepsilon}\overline{\nabla_y^{NC} v} \quad \text{and} \quad \nabla^{NC}\overline{v} = \frac{1}{\varepsilon}\overline{\nabla_y^{NC} v}$$

or in short by

$$\nabla\overline{v} = \overline{\nabla_x^C v} + \frac{1}{\varepsilon}\overline{\nabla_y v}. \tag{73}$$

Finally, the approximations (69) and (70) still hold.

A.4. Approximations of the two-scale transform of the derivatives

Consider an εY-periodic set $\omega_1 \subset \omega$ which is connected in the d^C directions x^C. The superscript C refers to the directions of connectivity whereas NC will refer to the direction with no connectivity. The part of the boundary $\partial\omega$ where the unit outward normal vector $n_x^C \neq 0$ is divided into γ_0^M, where boundary conditions are imposed and γ_1^M. It is the part of the boundary where the connection between adjacent cells occurs.

First-order derivatives: Let u be a function defined on ω_1, depending on the parameter ε, vanishing on $\gamma_0^M \cap \gamma_1$ and such that its norms $\|u\|_{\omega_1}$ and $\|\nabla u\|_{\omega_1}$ are $O(1)$ with respect to ε. From the norm conservation through the two-scale transform, we already know that $\|\widehat{u}\|_{\omega\times Y_1}$ and $\|\widehat{\nabla u}\|_{\omega\times Y_1}$ are also $O(1)$. If, in any manner, it is known that $\widehat{u}$ admits an expansion with respect to ε on the form $\widehat{u}=u^0+\varepsilon\widetilde{u}^1+\varepsilon O(\varepsilon)$, at least in the weak sense, with u^0 and $\widetilde{u}^1$ independent of ε, then $u^0=0$ on γ_0^M, $\nabla_y u^0=0$ on $\omega\times Y_1$,

$$\widehat{\nabla u}=\nabla_x^C u^0+\nabla_y u^1+O(\varepsilon)\quad \text{on } \omega\times Y_1 \tag{74}$$

in the weak sense, $u^1=\widetilde{u}^1-y^C.\nabla_x^C u^0$, u^1 is Y-periodic on γ_{per}, $u^0\in L^2(\omega)$, $\nabla_x^C u^0(x)\in L^2(\omega)^d$, $u^1\in L^2(\omega\times Y_1)$ and $\nabla_y u^1\in L^2(\omega\times Y_1)^d$.

Second-order derivatives: In addition, we assume that $\|\nabla\nabla^{\mathrm{T}}u\|_{\omega_1}$ is $O(1)$, that $\nabla u=0$ on $\gamma_0^M\cap\gamma_1$ and that $\widehat{u}=u^0+\varepsilon\widetilde{u}^1+\varepsilon^2\widetilde{u}^2+\varepsilon^2 O(\varepsilon)$, at least in the weak sense. It then follows that $\|\widehat{\nabla\nabla^{\mathrm{T}}u}\|_{\omega\times Y_1}$ is $O(1)$, $\nabla_x u^0=0$ on γ_0^M, $\nabla_y\nabla_y^{\mathrm{T}}u^1=0$, $\nabla_y^C u^1=0$,

$$\begin{aligned}&\widehat{\nabla u}=\nabla_x^C u^0+\theta^{NC}+O(\varepsilon)\\ &\text{and}\quad \widehat{\nabla\nabla^{\mathrm{T}}u}=\nabla_x^C(\nabla_x^C)^{\mathrm{T}}u^0+\nabla_x^C(\theta^{NC})^{\mathrm{T}}+(\nabla_x^C(\theta^{NC})^{\mathrm{T}})^{\mathrm{T}}+\nabla_y\nabla_y^{\mathrm{T}}u^2+O(\varepsilon)\end{aligned} \tag{75}$$

on $\omega\times Y_1$ in the weak sense, $u^2=\widetilde{u}^2-y^C.\nabla_x^C\widetilde{u}^1+(y^C.\nabla_x^C)^2u^0$, u^2 and $\nabla_y u^2$ are Y-periodic on γ_{per}, $\theta^{NC}=\nabla_y^{NC}u^1$, which is independent of y, $\nabla_x^C(\nabla_x^C)^{\mathrm{T}}u^0\in L^2(\omega)^{d\times d}$ and $\nabla_x^C\nabla_y u^1$, $\nabla_y\nabla_y^{\mathrm{T}}u^2\in L^2(\omega\times Y_1)^{d\times d}$.

Strong variations, first-order derivatives: In the case where the variations of u are sufficiently large so that $\|\nabla u\|_{\omega_1}$ is not of order $O(1)$ but $\|\varepsilon\nabla u\|_{\omega_1}$ is $O(1)$ and $\widehat{u}=u^0+O(\varepsilon)$, at least in the weak sense, then $\nabla_y u^0\in L^2(\omega\times Y_1)$ and

$$\varepsilon\widehat{\nabla u}(x,y)=\nabla_y u^0+O(\varepsilon) \tag{76}$$

in the weak sense.

Strong variations, second-order derivatives: If in addition $\|\varepsilon^2\nabla\nabla^{\mathrm{T}}u\|_{\omega_1}$ is $O(1)$ then $\nabla_y\nabla_y^{\mathrm{T}}u^0\in L^2(\omega\times Y_1)$ and

$$\varepsilon^2\widehat{\nabla\nabla^{\mathrm{T}}u}(x,y)=\nabla_y\nabla_y^{\mathrm{T}}u^0+O(\varepsilon). \tag{77}$$

Here we sketch the proof of these approximations by indicating the calculation steps without going into precise mathematical justifications.

Proof for the first-order derivative: The proof is decomposed into four steps.

(i) If $\|\nabla u\|_{\omega_1}$ is $O(1)$ then $\nabla_y u^0=0$. This comes from the properties of the two-scale transform recalled above: $\varepsilon\|\nabla u\|_{\omega_1}=\varepsilon\|\widehat{\nabla u}\|_{\omega\times Y_1}=\|\nabla_y\widehat{u}\|_{\omega\times Y_1}=O(\varepsilon)$.

Next, we decompose $\widehat{\nabla u}=\widehat{\nabla^C u}+\widehat{\nabla^{NC} u}$ and compute each part separately.

(ii) The first term turns out to be approximated by

$$\widehat{\nabla^C u}=\nabla_x^C u^0+\nabla_y^C u^1+O(\varepsilon)\quad \text{on } \omega\times Y_1.$$

Consider a function $v(x,y)$ two times continuously differentiable with respect to x in $\omega\times Y_1$, vanishing for $y\in\partial Y_1-\gamma_{\text{per}}$ and for $x\in\gamma_1^M$ and extended by zero for $y\in Y-Y_1$. We assume also that the function $\overline{v}$ defined from v by (71) is differentiable with respect to y. Then, E_{ω_1} denoting the operator of extension by zero from ω_1 to ω,

$$X=\int_{\omega\times Y}TE_{\omega_1}\nabla^C u.v\,\mathrm{d}y\mathrm{d}x=\int_{\omega_1}\nabla^C u.T^*v\mathrm{d}x=\int_{\omega_1}\nabla^C u.\overline{v}\mathrm{d}x+O(\varepsilon)$$

due to the zero-order approximation of T^*v by $\overline{v}$ and the fact that $\|\nabla u\|_{\omega_1}$ is bounded. Applying the Green formula and taking into account that the product uv vanishes on the boundary of ω it follows that

$$X=-\int_{\omega_1}u(\overline{\mathrm{div}_x^C v}+\varepsilon^{-1}\overline{\mathrm{div}_y^C v})\mathrm{d}x+O(\varepsilon).$$

Applying the approximation (64) at the zero order to $\overline{\mathrm{div}_x^C v}$ and at the first order to $\overline{\mathrm{div}_y^C v}$ yields

$$X=-\int_{\omega_1}uT^*(\mathrm{div}_x^C v+\varepsilon^{-1}\mathrm{div}_y^C v+y^C.\nabla_x^C\mathrm{div}_y^C v)\mathrm{d}x+O(\varepsilon)$$

or equivalently

$$X = -\int_{\omega\times Y_1} \widehat{u}(\operatorname{div}_x^C v + \varepsilon^{-1}\operatorname{div}_y^C v + y^C.\nabla_x^C \operatorname{div}_y^C v)\mathrm{d}x\mathrm{d}y + O(\varepsilon).$$

Since $\widehat{u} = u^0 + \varepsilon\widetilde{u}^1 + \varepsilon O(\varepsilon)$ and $\nabla_y^C u^0 = 0$, applying the Green formula in the reverse sense yields

$$\begin{aligned}\int_{\omega\times Y} \widehat{\nabla^C u}.v\mathrm{d}y\mathrm{d}x &= \int_{\omega\times Y_1} (\nabla_x^C u^0 + \nabla_y^C u^1).v\mathrm{d}y\mathrm{d}x \\ &- \int_{\omega\times\gamma_{\mathrm{per}}} u^1 v.n_y^C \mathrm{d}s(y)\mathrm{d}x - \int_{\gamma_0^M\times Y_1} u^0 v.n_x^C \mathrm{d}y\mathrm{d}s(x) + O(\varepsilon)\end{aligned} \tag{78}$$

with $u^1 = \widetilde{u}^1 - y^C.\nabla_x^C u^0$. From the conditions imposed on v, it follows that all the boundary terms except those on $\omega\times\gamma_{\mathrm{per}}$ vanish. Here we have used the fact that $\int_{Y_1} u^0 y^{NC}.\nabla_x \operatorname{div}_y^C v\mathrm{d}y = 0$. Reducing the choice of functions to those satisfying $v = 0$ on $\omega\times\gamma_{\mathrm{per}}$ and on $\gamma_0^M \times Y_1$ gives

$$\int_{\omega\times Y} \widehat{\nabla^C u}.v\mathrm{d}y\mathrm{d}x = \int_{\omega\times Y_1} (\nabla_x^C u^0 + \nabla_y^C u^1).v\mathrm{d}y\mathrm{d}x + O(\varepsilon)$$

which holds only for the above-mentioned v. However, from a density argument this is valid also for all $v \in L^2(\omega\times Y_1)$. So we conclude that the equality $\widehat{\nabla^C u} = \nabla_x^C u^0 + \nabla_y^C u^1 + O(\varepsilon)$ holds in the weak sense.

(iii) As a by-product of (78) it follows that u^1 is Y-periodic on γ_{per} and $u^0 = 0$ on γ_0^M. Restarting from (78) with $v = 0$ on $\gamma_0^M \times Y_1$ it follows that

$$\int_{\omega\times\gamma_{\mathrm{per}}} u^1 v.n_y^C \mathrm{d}s(y)\mathrm{d}x = O(\varepsilon)$$

which says that u^1 is Y-periodic on γ_{per}. Finally for any v there remains

$$\int_{\gamma_0^M\times Y_1} u^0 v.n_x^C \mathrm{d}s(y)\mathrm{d}x = O(\varepsilon)$$

which says that $u^0 = 0$ on γ_0^M.

(iv) The expression of the complementary $\widehat{\nabla^{NC} u}$ is

$$\widehat{\nabla^{NC} u} = \nabla_y^{NC} u^1 + O(\varepsilon).$$

Indeed $\widehat{\nabla^{NC} u} = \varepsilon^{-1}\nabla_y^{NC}\widehat{u} = \varepsilon^{-1}\nabla_y^{NC}(u^0 + \varepsilon\widetilde{u}^1) + O(\varepsilon) = \nabla_y^{NC} u^1 + O(\varepsilon)$.

This completes the derivation of (74).

Sketch of the proof for the second-order derivative: From $\|\nabla\nabla^{\mathrm{T}} u\|_{\omega_1} = O(1)$ it follows that $\nabla_y \nabla_y^{\mathrm{T}} u^1$ vanishes; then u^1 is affine with respect to y and $\theta^{NC} = \nabla_y^{NC} u^1$ is independent of y. Furthermore, u^1 being periodic on γ_{per} implies that it is independent of y^C or in other words that $\nabla_y^C u^1 = 0$. The proof of (75) follows the same arguments that for the proof of (74) except that v is a symmetric $d\times d$ matrix. The matrix of the second-order derivative splits in four parts: $\nabla\nabla^{\mathrm{T}} u = \nabla^C(\nabla^C)^{\mathrm{T}} u + \nabla^C(\nabla^{NC})^{\mathrm{T}} u + \nabla^{NC}(\nabla^C)^{\mathrm{T}} u + \nabla^{NC}(\nabla^{NC})^{\mathrm{T}} u$.

(i) The approximation of the first term

$$\widehat{\nabla^C(\nabla^C)^{\mathrm{T}} u} = \nabla_x^C(\nabla_x^C)^{\mathrm{T}} u^0 + \nabla_y^C(\nabla_y^C)^{\mathrm{T}} u^2 + O(\varepsilon) \quad \text{on } \omega\times Y_1 \tag{79}$$

and of the boundary conditions on γ_0^M and on γ_{per} are derived through the same calculation. The second-order approximation (64) of $T^* v$ leads, after few lines of simple calculation, to

$$\begin{aligned}\int_{\omega\times Y} \widehat{\nabla^C(\nabla^C)^{\mathrm{T}} u} :: v\mathrm{d}y\mathrm{d}x &= \int_{\omega\times Y_1} (\nabla_x^C(\nabla_x^C)^{\mathrm{T}} u^0 + \nabla_y^C(\nabla_y^C)^{\mathrm{T}} u^2) :: v\mathrm{d}y\mathrm{d}x \\ &+ \int_{\omega\times\gamma_{\mathrm{per}}} [u^1(\operatorname{div}_x^C v) + u^2(\operatorname{div}_y^C v) - (\nabla_y^C u^2)^{\mathrm{T}} v].n_y^C \mathrm{d}s(y)\mathrm{d}x + O(\varepsilon).\end{aligned}$$

Please cite this article in press as: M. Lenczner, R.C. Smith, A two-scale model for an array of AFM's cantilever in the static case, Mathematical and Computer Modelling (2007), doi:10.1016/j.mcm.2006.12.028

The formula (79) as well as the boundary conditions follow.

(ii) The second term $\nabla^C \widehat{\nabla^{NC}} u$ is approximated by

$$\nabla^C \widehat{(\nabla^{NC})}^{\mathrm{T}} u = \nabla_x^C (\theta^{NC})^{\mathrm{T}} + \nabla_y^{NC} (\nabla_y^C)^{\mathrm{T}} u^2 + O(\varepsilon). \tag{80}$$

Here ∇^{NC} is applied to u and ∇^C is transposed on the test function. Following the calculation and using the fact that $\nabla_y^{NC}(y^C.\nabla_x^C u^0) = 0$ the formula

$$\int_{\omega\times Y} \nabla^C \widehat{(\nabla^{NC})}^{\mathrm{T}} u :: v \mathrm{d}y\mathrm{d}x = \int_{\omega\times Y_1} (\nabla_x^C (\theta^{NC})^{\mathrm{T}} + \nabla_y^{NC} (\nabla_y^C)^{\mathrm{T}} u^2) :: v \mathrm{d}y\mathrm{d}x + O(\varepsilon)$$

arises when $v = 0$ on $\omega \times \gamma_{\mathrm{per}}$ and on $\partial\omega \times Y_1$. This immediately provides (80).

(iii) The third term $\nabla^{NC} \widehat{(\nabla^C)}^{\mathrm{T}} u$ is equal to the second term transposed so its approximation is equal to the transposed approximation of the second term.

(iv) The derivation of the formula for the fourth term

$$\nabla^{NC} \widehat{(\nabla^{NC})}^{\mathrm{T}} u = \nabla_y^{NC} (\nabla_y^{NC})^{\mathrm{T}} u^2 + O(\varepsilon) \quad \text{on } \omega \times Y_1 \tag{81}$$

is straightforward.

Proof for the strong variations case: For proving (76) and (77), let us recall that $\varepsilon \widehat{\nabla u} = \nabla_y \widehat{u}$ and $\varepsilon^2 \widehat{\nabla\nabla^{\mathrm{T}} u} = \nabla_y \nabla_y^{\mathrm{T}} \widehat{u}$, so using the expansion of $\widehat{u}$ leads directly to the results.

A.5. An inequality

Lemma 1. *The inequality*

$$\|v\|_{\omega_P} \le C \|\chi_{\omega_B} \nabla v + \chi_{\omega_F} \varepsilon \nabla v\|_{\omega_P} \tag{82}$$

is satisfied for all $v \in H^1(\omega_P)$ such that $v = 0$ on γ_0^ε it follows that

Proof. (i) First we establish that there exists a constant $C_1 > 0$ such that for all $v \in H^1(Y) \|v\|_{Y_C}^2 \le C_1(\|v\|_{Y_B}^2 + \|\nabla v\|_Y^2)$. This is proven similarly to the classical Poincaré inequalities.

(ii) Then we establish that there exists a constant $C_2 > 0$ such that for all $v \in H^1_{\gamma_0^\varepsilon}(\omega_P)$, $\|v\|_{\omega_P}^2 \le C_3 \|\chi_{\omega_B}(\partial_{x_1} v, \varepsilon\partial_{x_2} v) + \varepsilon\nabla v\|_{\omega_P}^2$ uniformly with respect to $\varepsilon > 0$. Let us start from the previous inequality and, for each i, let us apply the change of variable that maps Y towards Y_i^ε. This leads to a family of inequality that we sum over i. It follows that for all $v \in H^1(\omega_P)$:

$$\|v\|_{\omega_C}^2 \le C_1(\|v\|_{\omega_C}^2 + \|\varepsilon\nabla v\|_{\omega_P}^2). \tag{83}$$

By another way, let us introduce a scaling of ω_B by a factor of $n = 1/\varepsilon$ in the direction x_2 only. This leads to a family $\widehat{\omega}$ of n strips with length equal to 1 in the x_1 direction and of the order of one in the second direction. The classical Poincaré inequality may be applied to each of them, which in turn by summation over the n strips yields $\|v\|_{\widehat{\omega}}^2 \le C_2 \|\nabla v\|_{\widehat{\omega}}^2$ provided that $v \in H^1_{\widehat{\gamma}_0^\varepsilon}(\widehat{\omega}^\varepsilon)$. Here $\widehat{\gamma}_0^\varepsilon$ is obtained through the dilatation of γ_0^ε by a factor $1/\varepsilon$. By reversing the scaling, it follows that for all $v \in H^1_{\gamma_0^\varepsilon}(\omega)$,

$$\|v\|_{\omega_C}^2 \le C_2 \|(\partial_{x_1} v, \varepsilon\partial_{x_2} v)\|_{\omega_C}^2. \tag{84}$$

Combining (83) and (84) yields (ii).

(iii) The desired result is a direct consequence of (ii). ■

References

[1] P. Destuynder, M. Salaun, Mathematical Analysis of Thin Plate Models, Springer, Berlin, 1996.
[2] P.G. Ciarlet, Mathematical Elasticity, vol. II, North-Holland, Amsterdam, 1997.

[3] E. Sanchez-Palencia, Nonhomogeneous Media; Vibration Theory, in: Lecture Notes in Phys., vol. 127, Springer, Berlin, 1980.
[4] A. Bensoussan, J.-L. Lions, G. Papanicolaou, Asymptotic Analysis for Periodic Structures, North-Holland, Amsterdam, 1978.
[5] G. Allaire, SIAM Journal on Mathematical Analysis 23 (6) (1992) 1482–1518.
[6] E. Canon, M. Lenczner, Mathematical and Computer Modelling 26 (5) (1997) 79–106.
[7] G. Nguetseng, SIAM Journal on Mathematical Analysis 20 (3) (1989) 608–623.
[8] D. Cioranescu, A. Damlamian, G. Griso, Comptes Rendus Mathématique Académic des Sciences Paris 335 (1) (2002) 99–104.
[9] J. Casado-Diaz, Two-scale convergence for nonlinear Dirichlet problems in perforated domains, Proceedings of the Royal Society of Edinburgh. Section A 130 (2) (2000) 249–276.
[10] M. Lenczner, D. Mercier, Multiscale Modeling & Simulation 2 (3) (2004) 359–397.
[11] M. Lenczner, G. Senouci-Bereksi, Mathematical Models & Methods in Applied Sciences 9 (6) (1999) 899–932.
[12] R.F. Fung, S. Huang, Dynamic modeling; vibration analysis of the atomic force microscope, Transactions of the ASME, Journal of Vibration and Acoustics 123 (4) (2001) 502–509.
[13] D. Drakova, Theoretical modelling of scanning tunnelling microscopy, scanning tunnelling spectroscopy; atomic force microscopy, Reports on Progress in Physics 64 (2) (2001) 205–290.
[14] F.J. Giessibl, Advances in atomic force microscopy, Reviews of Modern Physics 75 (3) (2003) 949–983.
[15] M. Lenczner, Homogenization of an electric circuit, Comptes Rendus de l'Academie des Sciences, Serie II 324 (9) (1997) 537–542.
[16] R.W. Stark, G. Schitter, M. Stark, R. Guckenberger, A. Stemmer, State-space model of freely vibrating and surface-coupled cantilever dynamics in atomic force microscopy, Physical Review B (Condensed Matter and Materials Physics) 69 (8) (2004) 85412-1-9.
[17] B. Gotsmann, C. Seidel, B. Anczykowski, H. Fuchs, Conservative and dissipative tip-sample interaction forces probed with dynamic AFM, Physical Review B (Condensed Matter) 60 (15) (1999) 11051–11061.
[18] O.I. Vinogradova, H.-J. Butt, G.E. Yakubov, F. Feuillebois, Dynamic effects on force measurements. I. Viscous drag on the atomic force microscope cantilever, Review of Scientific Instruments 72 (5) (2001) 2330–2339.
[19] N. Lobontiu, E. Garcia, Two microcantilever designs: Lumped-parameter model for static and modal analysis, Journal of Microelectromechanical Systems 13 (1) (2004) 41–50.
[20] N. Jalili, M. Dadfarnia, D.M. Dawson, A fresh insight into the microcantilever-sample interaction problem in non-contact atomic force microscopy, Transactions of the ASME, Journal of Dynamic Systems, Measurement and Control 126 (2) (2004) 327–335.
[21] R. Garcia, R. Perez, Dynamic atomic force microscopy methods, Surface Science Reports 47 (6–8) (2002) 197–301.
[22] F.-J. Elmer, M. Dreier, Eigenfrequencies of a rectangular atomic force microscope cantilever in a medium, Journal of Applied Physics 81 (12) (1997) 7709–7714.
[23] J.E. Sader, Frequency response of cantilever beams immersed in viscous fluids with applications to the atomic force microscope, Journal of Applied Physics 84 (1) (1998) 64–76.
[24] M. Napoli, W. Zhang, K. Turner, B. Bamieh, Characterization of electrostatically coupled microcantilevers, Journal of Microelectromechanical Systems 14 (2) (2005) 295–304.
[25] M. Napoli, B. Bamieh, M. Dahleh, Optimal control of arrays of microcantilevers, Transactions of the ASME, Journal of Dynamic Systems, Measurement and Control 121 (4) (1999) 686–690.
[26] C. Argento, R.H. French, Parametric tip model and force–distance relation for Hamaker constant determination from atomic force microscopy, Journal of Applied Physics 11 (1) (1996) 6081–6090.
[27] C. Argento, A. Jagota, W.C. Carter, Surface formulation for molecular interactions of macroscopic bodies, Journal of the Mechanics and Physics of Solids 45 (7) (1997) 1161–1183.
[28] J. Israelachvili, Intermolecular and Surface Forces, second ed., Academic Press, London, 1992.
[29] H.P. Lang, M. Hegner, C. Gerber, Cantilever array sensors, Materials Today 8 (4) (2005) 30–36.
[30] R.J. Fasching, Y. Tao, F.B. Prinz, Cantilever tip probe arrays for simultaneous SECM and AFM analysis, Sensors and Actuators, B: Chemical 108 (1–2) (2005) 964–972.
[31] N. Nugaeva, K.Y. Gfeller, N. Backmann, H.P. Lang, M. Duggelin, M. Hegner, Micromechanical cantilever array sensors for selective fungal immobilization and fast growth detection, Biosensors and Bioelectronics 21 (6) (2005) 849–856.
[32] T. Volden, M. Zimmermann, D. Lange, O. Brand, H. Baltes, Dynamics of CMOS-based thermally actuated cantilever arrays for force microscopy, Sensors and Actuators, A: Physical 115 (22) (2004) 516–552.
[33] T. Xu, M. Bachman, F. Zeng, G. Li, Polymeric micro-cantilever array for auditory front-end processing, Sensors and Actuators, A: Physical 114 (2–3) (2004) 176–182.
[34] Z. Yang, X. Li, Y. Wang, H. Bao, M. Liu, Micro cantilever probe array integrated with Piezoresistive sensor, Microelectronics Journal 35 (5) (2004) 479–483.
[35] Y. Kim, H. Nam, S. Cho, J. Hong, D. Kim, J.U. Bu, PZT cantilever array integrated with piezoresistor sensor for high speed parallel operation of AFM, Sensors and Actuators, A: Physical 103 (1–2) (2003) 122–129.
[36] D. Saya, K. Fukushima, H. Toshiyoshi, G. Fujita, H. Kawakatsu, Fabrication of single-crystal Si cantilever array, Sensors and Actuators, A: Physical 95 (2–3) (2002) 281–287.
[37] B.H. Kim, F.E. Prins, D.P. Kern, S. Raible, U. Weimar, Multicomponent analysis and prediction with a cantilever array based gas sensor, Sensors and Actuators, B: Chemical 78 (1–3) (2001) 12–18.
[38] F.M. Battiston, J.-P. Ramseyer, H.P. Lang, M.K. Baller, C. Gerber, J.K. Gimzewski, E. Meyer, H.-J. Guntherodt, A chemical sensor based on a microfabricated cantilever array with simultaneous resonance-frequency and bending readout, Sensors and Actuators, B: Chemical 77 (1–2) (2001) 122–131.
[39] E.M. Chow, H.T. Soh, H.C. Lee, J.D. Adams, S.C. Minne, G. Yaralioglu, A. Atalar, C.F. Quate, T.W. Kenny, Integration of through-wafer interconnects with a two-dimensional cantilever array, Sensors and Actuators, A: Physical A83 (1–3) (2000) 118–123.

Please cite this article in press as: M. Lenczner, R.C. Smith, A two-scale model for an array of AFM's cantilever in the static case, Mathematical and Computer Modelling (2007), doi:10.1016/j.mcm.2006.12.028

[40] R.G. Rudnitsky, E.M. Chow, T.W. Kenny, Rapid biochemical detection and differentiation with magnetic force microscope cantilever arrays, Sensors and Actuators, A: Physical A83 (1–3) (2000) 256–262.
[41] M.K. Baller, H.P. Lang, J. Fritz, Ch. Gerber, J.K. Gimzewski, U. Drechsler, H. Rothuizen, M. Despont, P. Vettiger, F.M. Battiston, J.P. Ramseyer, P. Fornaro, E. Meyer, H.-J. Guntherodt, Cantilever array-based artificial nose, Ultramicroscopy 82 (1) (2000) 1–9.
[42] M. Lutwyche, C. Andreoli, G. Binnig, J. Brugger, U. Drechsler, W. Haberle, H. Rohrer, H. Rothuizen, P. Vettiger, G. Yaralioglu, C. Quate, 5×5 2D AFM cantilever arrays a first step towards a Terabit storage device, Sensors and Actuators, A: Physical A73 (1–2) (1999) 89–94.
[43] Y.-S. Kim, S.C. Lee, W.-H. Jin, S. Jang, H.-J. Nam, J.-U. Bu, 100×100 thermo-piezoelectric cantilever array for SPM nano-data-storage application, Sensors and Materials 17 (2) (2005) 57–63.
[44] K. Kakushima, T. Watanabe, K. Shimamoto, T. Gouda, M. Ataka, H. Mimura, Y. Isono, G. Hashiguchi, Y. Mihara, H. Fujita, Japanese Journal of Applied Physics 43 (6B) (2004) 4041–4044.
[45] M.J. Graf, C.P. Opeil, T.E. Huber, Magnetic anisotropy and de Haas-van Alphen oscillations in a Bi microwire array studied via cantilever magnetometry at low temperatures, Journal of Low Temperature Physics 134 (5–6) (2004) 1055–1068.
[46] X. Yu, D. Zhang, T. Li, X. Wang, Y. Ruan, X. Du, Fabrication and analysis of micromachined cantilever array, Chinese Journal of Semiconductors 24 (8) (2003) 861–865.
[47] P. Srinivasan, F.R. Beyette Jr., I. Papautsky, Micromachined arrays of cantilevered glass probes, Applied Optics 43 (4) (2004) 776–782.
[48] D. Bullen, S.-W. Chung, X. Wang, J. Zou, C.A. Mirkin, C. Liu, Parallel dip-pen nanolithography with arrays of individually addressable cantilevers, Applied Physics Letters 84 (5) (2004) 789–791.
[49] M. Calleja, J. Tamayo, A. Johansson, P. Rasmussen, L.M. Lechuga, A. Boisen, Polymeric cantilever arrays for biosensing applications, Sensor Letters 1 (1) (2003) 20–24.
[50] N. Abedinov, C. Popov, Z. Yordanov, T. Ivanov, T. Gotszalk, P. Grabiec, W. Kulisch, I.W. Rangelow, D. Filenko, Yu. Shirshov, Chemical recognition based on micromachined silicon cantilever array, Journal of Vacuum Science and Technology B 21 (6) (2003) 2931–2936.
[51] D. Dragoman, M. Dragoman, Biased micromechanical cantilever arrays as optical image memory, Applied Optics 42 (8) (2003) 1515–1519.
[52] Y. Arntz, J.D. Seelig, H.P. Lang, J. Zhang, P. Hunziker, J.P. Ramseyer, E. Meyer, M. Hegner, C. Gerber, Label-free protein assay based on a nanomechanical cantilever array, Nanotechnology 14 (1) (2003) 86–90.
[53] T.E. Schaffer, Force spectroscopy with a large dynamic range using small cantilevers and an array detector, Journal of Applied Physics 91 (7) (2002) 4739.
[54] N. Abedinov, P. Grabiec, T. Gotszalk, Tz. Ivanov, J. Voigt, I.W. Rangelow, Micromachined piezoresistive cantilever array with integrated resistive microheater for calorimetry and mass detection, Journal of Vacuum Science and Technology, Part A: Vacuum, Surfaces and Films 19 (6) (2001) 2884–2888.
[55] H.-M. Cheng, M.T.S. Ewe, G.T.-C. Chiu, R. Bashir, Modeling and control of piezoelectric cantilever beam micro-mirror and micro-laser arrays to reduce image banding in electrophotographic processes, Journal of Micromechanics and Microengineering 11 (5) (2001) 487–498.
[56] J.D. Green, G.U. Lee, Atomic force microscopy with patterned cantilevers and tip arrays: Force measurements with chemical arrays, Langmuir 16 (8) (2000) 4009–4015.
[57] Y. Min, H. Lin, D.E. Dedrick, S. Satyanarayana, A. Majumdar, A.S. Bedekar, J.W. Jenkins, S. Sundaram, A 2-D microcantilever array for multiplexed biomolecular analysis, Journal of Microelectromechanical Systems 13 (2) (2004) 290–299.
[58] U. Drechsler, N. Burer, M. Despont, U. Durig, B. Gotsmann, F. Robin, P. Vettiger, Cantilevers with nano-heaters for thermomechanical storage application, Microelectronic Engineering 67–68 (2003) 397–404.
[59] F. Tian, K.M. Hansen, T.L. Ferrell, T. Thundat, D.C. Hansen, Dynamic microcantilever sensor for discerning biomolecular interactions, Analytical Chemistry 77 (6) (2005) 1601–1606.
[60] K.M. Hansen, H.-F. Ji, G. Wu, R. Datar, R. Cote, A. Majumdar, T. Thundat, Cantilever-based optical deflection assay for discrimination of DNA single-nucleotide mismatches, Analytical Chemistry 73 (7) (2001) 1567–1571.
[61] J. Pepper, R. Noring, M. Klempner, B. Cunningham, A. Petrovich, R. Bousquet, C. Clapp, J. Brady, B. Hugh, Detection of proteins and intact microorganisms using microfabricated flexural plate silicon resonator arrays, Sensors and Actuators, B: Chemical 96 (3) (2003) 565–575.
[62] W.P. King, T.W. Kenny, K.E. Goodson, G.L.W. Cross, M. Despont, U.T. Durig, H. Rothuizen, G. Binnig, P. Vettiger, Design of atomic force microscope cantilevers for combined thermomechanical writing and thermal reading in array operation, Journal of Microelectromechanical Systems 11 (6) (2002) 765–774.